



SERVIÇO PÚBLICO FEDERAL  
MINISTÉRIO DA EDUCAÇÃO  
UNIVERSIDADE FEDERAL DE UBERLÂNDIA  
FACULDADE DE ODONTOLOGIA  
PROGRAMA DE PÓS-GRADUAÇÃO EM ODONTOLOGIA

Airin Karelys Avendaño Rondon

Fluxo digital na confecção de protetores bucais – Efeito nas propriedades mecânicas, adaptação e desempenho biomecânico.

*Digital workflow used for custom-fit mouthguards fabrication – Effect on the mechanical properties, adaptation, and biomechanical performance.*

Dissertação apresentada à Faculdade de Odontologia da Universidade Federal de Uberlândia como requisito parcial para obtenção do Título de Mestre em Odontologia na área de Clínica Odontológica Integrada.

Uberlândia, 2024

Airin Karelys Avendaño Rondon

**Fluxo digital na confecção de protetores bucais – Efeito nas propriedades mecânicas, adaptação e desempenho biomecânico.**

*Digital workflow used for custom-fit mouthguards fabrication – Effect on the mechanical properties, adaptation, and biomechanical performance.*

Dissertação apresentada à Faculdade de Odontologia da Universidade Federal de Uberlândia como requisito parcial para obtenção do Título de Mestre em Odontologia na área de Clínica Odontológica Integrada.

Orientador: Prof. Dr. Carlos José Soares

Banca Examinadora:

Prof. Dr. Carlos José Soares (UFU)

Profa. Dra. Priscilla Ferreira Soares (UFU)

Prof. Dr. Victor Setien (ULA)

Suplente

Prof. Dr. Luis Raposo (UFU)

Prof. Dr. Juan Pablo Pérez (ULA)

Uberlândia, 2024



**UNIVERSIDADE FEDERAL DE UBERLÂNDIA**  
Coordenação do Programa de Pós-Graduação em Odontologia  
Av. Pará, 1720, Bloco 4L, Anexo B, Sala 35 - Bairro Umuarama, Uberlândia-MG, CEP  
38400-902  
Telefone: (34) 3225-8115/8108 - www.ppgoufu.com - copod@umuarama.ufu.br



## ATA DE DEFESA - PÓS-GRADUAÇÃO

Programa de Pós-Graduação em:	Odontologia				
Defesa de:	Dissertação de Mestrado Acadêmico, nº 451, PPGODONTO				
Data:	Cinco de Julho de Dois Mil e Vinte e Quatro	Hora de início:	16:00	Hora de encerramento:	17:45
Matrícula do Discente:	12222ODO001				
Nome do Discente:	Airin Karelys Avendaño Rondón				
Título do Trabalho:	Fluxo digital na confecção de protetores bucais - Efeito nas propriedades mecânicas adaptação e desempenho biomecânico				
Área de concentração:	Clínica Odontológica Integrada				
Linha de pesquisa:	Biomecânica Aplicada à Odontologia				
Projeto de Pesquisa de vinculação:	Biomecânica Aplicada à Odontologia				

Reuniu-se n o Anfiteatro/Sala 23 Bloco 4L - Anexo A Campus Umuarama, da Universidade Federal de Uberlândia, a Banca Examinadora, designada pelo Colegiado do Programa de Pós-graduação em Odontologia, assim composta: Professores Doutores: Victor José Setien Duin (UNIVERSIDAD DE LOS ANDES), participou da defesa de Dissertação por meio de vídeo conferência desde a cidade de Mérida/Venezuela; Priscilla Barbosa Ferreira Soares (UFU); Carlos José Soares (UFU); orientador(a) do(a) candidato(a).

Iniciando os trabalhos o(a) presidente da mesa, Dr(a). Carlos José Soares, apresentou a Comissão Examinadora e o candidato(a), agradeceu a presença do público, e concedeu ao Discente a palavra para a exposição do seu trabalho. A duração da apresentação do Discente e o tempo de arguição e resposta foram conforme as normas do Programa.

A seguir o senhor(a) presidente concedeu a palavra, pela ordem sucessivamente, aos(às) examinadores(as), que passaram a arguir o(a) candidato(a). Ultimada a arguição, que se desenvolveu dentro dos termos regimentais, a Banca, em sessão secreta, atribuiu o resultado final, considerando o(a) candidato(a):

Aprovado(a).

Esta defesa faz parte dos requisitos necessários à obtenção do título de Mestre.

O competente diploma será expedido após cumprimento dos demais requisitos, conforme as normas do Programa, a legislação pertinente e a regulamentação interna da UFU.

Nada mais havendo a tratar foram encerrados os trabalhos. Foi lavrada a presente ata que após lida e achada conforme foi assinada pela Banca Examinadora.



Documento assinado eletronicamente por **Carlos José Soares, Professor(a) do Magistério Superior**, em 05/07/2024, às 17:45, conforme horário oficial de Brasília, com fundamento no art. 6º, § 1º, do [Decreto nº 8.539, de 8 de outubro de 2015](#).



Documento assinado eletronicamente por **Priscilla Barbosa Ferreira Soares, Professor(a) do Magistério Superior**, em 05/07/2024, às 17:46, conforme horário oficial de Brasília, com fundamento no art. 6º, § 1º, do [Decreto nº 8.539, de 8 de outubro de 2015](#).



Documento assinado eletronicamente por **Víctor José Setién Duín, Usuário Externo**, em 05/07/2024, às 18:21, conforme horário oficial de Brasília, com fundamento no art. 6º, § 1º, do [Decreto nº 8.539, de 8 de outubro de 2015](#).



A autenticidade deste documento pode ser conferida no site [https://www.sei.ufu.br/sei/controlador\\_externo.php?acao=documento\\_conferir&id\\_orgao\\_acesso\\_externo=0](https://www.sei.ufu.br/sei/controlador_externo.php?acao=documento_conferir&id_orgao_acesso_externo=0), informando o código verificador **5510632** e o código CRC **3A064602**.

Ficha Catalográfica Online do Sistema de Bibliotecas da UFU  
com dados informados pelo(a) próprio(a) autor(a).

R771 2024	<p>Rondon, Airin Karelys Avendaño, 1994- Fluxo digital na confecção de protetores bucais – Efeito nas propriedades mecânicas, adaptação e desempenho biomecânico. [recurso eletrônico] : Digital workflow used for custom-fit mouthguards fabrication – Effect on the mechanical properties, adaptation, and biomechanical performance. / Airin Karelys Avendaño Rondon. - 2024.</p> <p>Orientador: Carlos José Soares. Dissertação (Mestrado) - Universidade Federal de Uberlândia, Pós-graduação em Odontologia. Modo de acesso: Internet. Disponível em: <a href="http://doi.org/10.14393/ufu.di.2024.449">http://doi.org/10.14393/ufu.di.2024.449</a> Inclui bibliografia. Inclui ilustrações.</p> <p>1. Odontologia. I. Soares, Carlos José, 1965-, (Orient.). II. Universidade Federal de Uberlândia. Pós- graduação em Odontologia. III. Título.</p> <p style="text-align: right;">CDU: 616.314</p>
--------------	--

Bibliotecários responsáveis pela estrutura de acordo com o AACR2:

Gizele Cristine Nunes do Couto - CRB6/2091  
Nelson Marcos Ferreira - CRB6/3074

## DEDICATÓRIA

### **A Deus;**

Agradeço, Deus, por seres meu guia constante! Agradeço por sempre ouvires minhas orações, desde o momento em que decidi deixar meu país para embarcar nesta jornada universitária. Nos momentos de maior dificuldade, senti Teu apoio incondicional e encontrei consolo em Tua presença. Agradeço profundamente pelas pessoas especiais que colocaste em minha vida, as quais me têm dado amor e apoio durante esses anos longe de casa. Pelas bênçãos recebidas e pelo que está por vir.

### **A meus pais, Freddy e Yoly**

Ao longo desta jornada acadêmica, o nosso amor incondicional e apoio constante têm sido a minha maior força. Esta apresentação é mais do que uma conquista pessoal; é o resultado do nosso sacrifício, paciência e fé em mim. A vocês dedico cada página escrita, cada descoberta e cada vitória alcançada. O nosso amor e orientação têm sido a luz que me tem guiado neste caminho rumo ao conhecimento. Com infinita gratidão, dedico vocês este feito, em reconhecimento a tudo o que fizeram por mim. Obrigado por serem os meus eternos motivadores e por me ensinarem o verdadeiro valor do esforço e dedicação.

### **A meus irmãos, Rebeca e Eduardo**

A vocês dedico esta conquista com gratidão infinita, reconhecendo o papel vital que desempenham na minha vida e no meu desenvolvimento acadêmico. O nosso amor, compreensão e cumplicidade têm sido a minha maior inspiração e motivação.

### **A Maribi,**

Por ser minha fonte constante de inspiração e apoio durante minha jornada acadêmica. Sua dedicação, sabedoria e encorajamento incondicional foram fundamentais para alcançar minhas metas. Sua influência deixou uma marca em minha vida, e por isso estarei eternamente grata. Você é mais do que uma professora; é uma mentora, uma guia e, acima de tudo, uma amiga.

## AGRADECIMENTOS

### **Ao Prof. Carlos Soares.**

Gostaria de expressar o meu mais sincero agradecimento pela sua orientação e apoio durante o processo do mestrado. Sua orientação e seus conselhos foram fundamentais nesse período. Sua dedicação me ensinou como abordar os desafios acadêmicos. Obrigada pela sua paciência, sabedoria e disposição para me oferecer seu tempo e conhecimento, por acreditar em mim, por me incentivar mesmo nos momentos mais difíceis e por ser um modelo a seguir em minha trajetória acadêmica.

### **À Professora Priscila Soares,**

Só tenho palavras de gratidão para lhe dirigir! Desde o início, você abriu portas para mim, me motivou e compreendeu, mesmo quando meu português não era o melhor. Admiro imensamente a profissional que você é, alguém que exerce sua profissão com paixão, que se esforça para acolher a todos e dar atenção a cada um. Obrigada por ser uma inspiração e por estar sempre presente para orientar e apoiar. Seu compromisso e dedicação são verdadeiramente admiráveis.

### **A Minha turma de mestrado**

Agradeço imensamente a todos vocês. Conviver, estudar e aprender ao lado de profissionais tão excelentes como vocês me fez crescer e evoluir significativamente ao longo deste mestrado. Conheci pessoas incríveis, fiz amizades e tenho certeza de que nossos caminhos continuarão se cruzando no futuro. Agradeço a cada um de vocês, e em especial a Bianca e Maria Tereza, muito obrigada, foi uma honra compartilhar essa experiência ao seu lado.

### **A OEA e GCUB**

Neste momento de conquista e gratidão, quero expressar meu mais sincero agradecimento pelo inestimável apoio financeiro que me foi concedido durante minha formação acadêmica. Espero que esse gesto de apoio seja retribuído multiplicado no benefício da sociedade à qual espero servir com os conhecimentos adquiridos.

## **A Universidad de Los Andes,**

Obrigada por me equipar com as habilidades, o conhecimento e a confiança necessários para alcançar meus objetivos e perseguir meus sonhos. Meu tempo nesta instituição foi verdadeiramente transformador e sempre levarei comigo as lições aprendidas e as memórias preciosas ao longo da minha vida.

## **A banca da qualificação**

Professor Luis Raposo, Professor Hugo Lemes, Professor Felipe Peres, suas orientações e sugestões foram muito importantes para o desenvolvimento deste trabalho. Agradeço por terem dedicado seu tempo e empenho para melhorar esta pesquisa em cada parte deste texto.

À Coordenação de Aperfeiçoamento de Pessoal de Nível Superior- Brasil (CAPES), ao Conselho Nacional de Desenvolvimento Científico e Tecnológico (CNPq; INCT Saúde Oral e Odontologia- Grants n. 406840/2022-9) e à Fundação de Amparo à Pesquisa do Estado de Minas Gerais (FAPEMIG # APQ-04262-22) – Brasil pela bolsa de mestrado e apoio financeiro que viabilizou a execução desta pesquisa



# Sumário

Abstract .....	25
Introdução e Referencial Teórico.....	26
Capítulos.....	28
CAPÍTULO 1.....	29
ARTIGO 1 .....	29
CAPÍTULO 2.....	38
ARTIGO 2 .....	38
Considerações Gerais .....	68
Referências .....	70

# Resumo

---

O uso de diferentes modelos para fabricação de protetores bucais personalizados (PBs) pode afetar nas propriedades mecânicas e características físicas do etileno acetato de vinila (EVA). Este estudo teve como objetivo avaliar o efeito do fluxo de trabalho digital sobre as propriedades físicas e mecânicas de protetores bucais customizados. O estudo foi dividido em 2 objetivos específicos: 1) Avaliar o efeito de diferentes materiais para modelos convencionais (gesso odontológico) ou modelos impressos em 3D nas propriedades físicas e mecânicas do EVA, e suas características de superfície. 2) Avaliar a adaptação, espessura e absorção de impacto dos PBs customizados de EVA produzidos usando modelos de gesso convencionais ou impressos 3D. No primeiro objetivo, placas de EVA foram plastificadas usando 4 tipos de modelos: Gesso tipo IV (GTIV), Gesso tipo IV resinoso (GTIVR), Resina 3D com tratamento (RI3DcT), Resina 3D sem tratamento de superfície (RI3DsT). Os EVAs plastificados foram cortados de acordo com a norma ISO 37-II ( $n = 30$ ) e usados para medir dureza Shore A, força máxima de ruptura,  $F$  (N), alongamento, EL (mm), e resistência máxima à ruptura, (MBS,MPa). Macrofotografia e microscopia eletrônica de varredura foram usadas para classificar a alteração da superfície do EVA. No objetivo 2, um modelo typodont com tecido gengival simulado foi utilizado como referência para a confecção de PB com dois materiais de modelos: Gesso tipo IV (GIV-PB) e resina impressa (3DPr-PB) ( $n = 10$ ), espessura do PB (mm), adaptação interna (mm) e área dos espaços vazios ( $\text{mm}^2$ ) entre as duas camadas de EVA foram mensuradas usando tomografia computadorizada de feixe cônico e o software Mimics (Materialize). A absorção de impacto do PB foi por meio do teste de extensometria durante impacto com pêndulo com uma esfera de aço em  $30^\circ$  sobre o modelo de typodont com e sem PBs. Os valores de Shore A diminuíram significativamente, independentemente do tipo de modelo. O modelo RI3DcT e o GtIV apresentaram valores mais altos de  $F$ , EL e MBS do que o GTIVRe o RI3DsT ( $p < 0,05$ ). O RI3DsT resulta em alteração grave da superfície do EVA e maior redução das propriedades mecânicas em contato com o modelo. O 3DPr-PB apresentou espessura semelhante ( $P = 0,371$ ), absorção de choque ao GIV-PB (87,0%) e melhor adaptação do GIV-MTG ( $P < 0,001$ ). O uso de revestimento de gel solúvel em água durante a pós-cura melhorou as propriedades mecânicas do EVA de forma semelhante quando plastificado sobre o modelo de gesso de pedra dental tipo IV. O 3DPr-PB apresentou desempenho semelhante ao do GIV-PB.

# Abstract

---

Using different models to fabricate custom mouthguards (MGs) can affect the mechanical properties and physical characteristics of ethylene vinyl acetate (EVA). This study aimed to evaluate the effect of the digital workflow on the physical and mechanical properties of customized mouthguards. The study was divided into 2 specific objectives: 1) Evaluate the impact of different materials for conventional models (dental stone) or 3D-printed models on EVA's physical and mechanical properties, and its surface characteristics. 2) Evaluate the adaptation, thickness, and impact absorption of customized EVA mouthguard thermoplastic materials (MTGs) produced using conventional or 3D-printed models. In the first objective, EVAs were plasticized using 4 types of models: Type IV dental stone (GTIV), Resinous Type IV dental stone (GTIVR), 3D resin with surface treatment (RI3DcT), and 3D resin without surface treatment (RI3DsT). The plasticized EVAs were cut according to ISO 37-II standard (n = 30) and used to measure Shore A hardness, maximum force of rupture (F, N), elongation (EL, mm), and maximum rupture strength (MBS, MPa). Macrophotography and scanning electron microscopy were used to classify the surface alteration of EVA. In objective 2, a typodont model with simulated gingival tissue was used as a reference for the fabrication of mouthguards with two model materials: Type IV dental stone (GIV-MTG) and 3D printed resin (3DPr-MTG) (n = 10). The thickness of the mouthguard (mm), internal adaptation (mm), and area of voids (mm<sup>2</sup>) between the two layers of EVA were measured using cone-beam computed tomography and Mimics software (Materialize). The impact absorption of the mouthguard was measured using a pendulum impact test with a steel ball at 30° on the typodont model with and without mouthguards. Shore A values decreased significantly, regardless of the model type. The RI3DcT model and GTIV showed higher values of F, EL, and MBS than GTIVR and RI3DsT (p < 0.05). RI3DsT resulted in severe surface alteration of EVA and greater reduction in mechanical properties in contact with the model. 3DPr-MTG showed similar thickness (P = 0.371), shock absorption to GIV-MTG (87.0%), and better adaptation than GIV-MTG (P < 0.001). The use of water-soluble gel coating during post-curing improved the mechanical properties of EVA similarly when plasticized over Type IV dental stone models. 3DPr-MTG performed similarly to GIV-MTG

# Introdução e Referencial Teórico

---

O traumatismo dentário é um dos problemas de saúde pública mais comuns, com prevalência que varia entre 15% a 23% em dentes decíduos e permanentes em todo o mundo.<sup>1,2</sup> As lesões orofaciais comuns em esportes incluem danos aos tecidos moles, lesões labiais, fraturas ósseas envolvendo a mandíbula, nasal e zigomático, e lesões dentárias, como fraturas, luxações e avulsões.<sup>3-5</sup>

Os protetores bucais previnem lesões decorrentes de traumas dentários, como fraturas e restaurações de dentes,<sup>6</sup> danos a estruturas adjacentes,<sup>7</sup> ao côndilo mandibular e ao disco articular.<sup>8</sup> e podem até mesmo prevenir tensões no germe permanente no caso de dentes decíduos.<sup>9</sup> Diferentes tipos de protetores bucais são descritos na literatura: pré-fabricados, termoplásticos (boil-and-bite) e feitos sob medida.<sup>10</sup>

De acordo com a American Society for Testing and Materials, no caso de prevenção de traumas dentários em esportes de alto impacto,<sup>11</sup> protetor bucal feito sob medida tem sido considerado padrão ouro em comparação com outros protetores bucais, devido à sua capacidade de proporcionar absorção de choque,<sup>12,13</sup> redução dos efeitos das forças geradas pelo impacto nas estruturas dentais e de suporte, e melhor ajuste.<sup>8,12</sup> O protetor bucal customizado oferece desempenho superior em termos de conforto, ajuste, estabilidade, respirabilidade, fonética e proteção das estruturas dentárias.<sup>13,14</sup>

O desempenho dos protetores bucais customizados depende de vários fatores, como o tipo de material utilizado para a sua confecção, geometria, processo de fabricação e espessura final do protetor bucal.<sup>15,16</sup> Vários estudos avaliaram diferentes materiais para a fabricação de protetores bucais personalizados,<sup>17</sup> demonstrando características ideais, como baixa absorção de água, dureza adequada, baixa incidência de delaminação,<sup>11,18</sup> e ótimas propriedades mecânicas.<sup>14</sup> No processo de fabricação de protetores bucais o copolímero de etileno e acetato de vinila (EVA) tem sido o material de primeira escolha.<sup>16,19,20</sup> Assim, é necessário obter um modelo que permita a reprodução da anatomia da arcada superior do atleta. Estes modelos podem ser obtidos, em primeiro lugar, por meio de moldes convencionais empregando, principalmente

alginate e modelos em gesso, considerados o padrão ouro.<sup>21</sup> Em segundo lugar, o aprimoramento de impressões digitais feitas com um scanner intraoral, tem permitido reduzir procedimentos clínicos e melhorar o conforto do paciente.<sup>22-24</sup> Nesse sentido, os escâneres intraorais permitem que as impressões digitais sejam usadas para fabricar modelos impressos e produzir protetores bucais personalizados a partir da laminação de EVA nesses modelos.

Entretanto, ainda é incerto se a termo plastificação do EVA em modelos impressos em resina pode comprometer as propriedades mecânicas, as características da superfície, a capacidade de absorção de impacto e o ajuste dos protetores bucais personalizados produzidos com EVA. Por isso, este estudo tem como objetivo avaliar por meio de dois estudos laboratoriais *in vitro* complementares o mecânico, as características físicas, o ajuste e a absorção de impactos dos protetores bucais personalizados fabricados com modelos obtidos em gesso e por impressão 3D.

# Capítulos

---

## CAPÍTULO 1

### ARTIGO 1

Effect of different materials for conventional and 3D-printed models on the mechanical properties of ethylene-vinyl acetate utilized for fabricating custom-fit mouthguards

Rondón AKA, Lozada MIT, Soares PBF, Raposo LHA, Soares CJ. Effect of different materials for conventional and 3D-printed models on the mechanical properties of ethylene-vinyl acetate utilized for fabricating custom-fit mouthguards. Dent Traumatol. 2023;00:1-8. doi: 10.1111/edt.12912.

# Effect of different materials for conventional and 3D-printed models on the mechanical properties of ethylene-vinyl acetate utilized for fabricating custom-fit mouthguards

Airin Karelys Avendaño Rondón<sup>1</sup> | Maribí Isomar Terán Lozada<sup>1</sup> |  
Priscilla Barbosa Ferreira Soares<sup>2</sup> | Luis Henrique Araujo Raposo<sup>3</sup> |  
Carlos José Soares<sup>4</sup>

<sup>1</sup>School of Dentistry, Federal University of Uberlândia, Uberlândia, Minas Gerais, Brazil

<sup>2</sup>Department of Periodontology and Implantology, School of Dentistry, Universidade de Uberlândia, Uberlândia, Minas Gerais, Brazil

<sup>3</sup>Department of Occlusion and Prosthodontic, School of Dentistry, Universidade de Uberlândia, Uberlândia, Minas Gerais, Brazil

<sup>4</sup>Department of Operative Dentistry and Dental Materials, School of Dentistry, Universidade de Uberlândia, Uberlândia, Minas Gerais, Brazil

## Correspondence

Carlos José Soares, Federal University of Uberlândia, School of Dentistry, Avenida Pará, 1720, Bloco 4L, anexo A, sala 42, Campos Umuarama, Uberlândia, Minas Gerais 38400-902, Brazil.  
Email: carlosjsoares@ufu.br

## Funding information

Conselho Nacional de Desenvolvimento Científico e Tecnológico; Coordenação de Aperfeiçoamento de Pessoal de Nível Superior; Fundação de Amparo à Pesquisa do Estado de Minas Gerais

## Abstract

**Background/Aim:** The interaction between the ethylene-vinyl acetate (EVA) with distinct materials utilized for obtaining dental models can affect the performance of resulting mouthguards. This study attempted to evaluate the effect of different materials for conventional (dental stone) or 3D-printed (resin) models on EVA's physical and mechanical properties and surface characteristics.

**Material and Methods:** EVA sheets (Bioart) were laminated over four model types: GIV, conventional Type IV dental stone model (Zhermack); ReG, resin-reinforced Type IV dental stone model (Zero Stone); 3DnT, 3D resin printed model (Anycubic) without surface treatment; 3DT, 3D-printed model (Anycubic) with water-soluble gel (KY Jelly Lubricant, Johnson & Johnson) coating during post-curing process. The EVA specimens were cut following the ISO 37-II standard ( $n = 30$ ). Shore A hardness was measured before and after plasticization on the contact (internal) or opposite (external) surfaces with the model. The breaking force (F, N), elongation (EL, mm), and ultimate tensile strength (UTS, MPa) were measured using a universal testing machine. Macro-photography and scanning electron microscopy were adopted for classifying the EVA surface alteration. Data were analyzed by one-way ANOVA with repeated measures, followed by Tukey's test ( $\alpha = .05$ ).

**Results:** Plasticization significantly decreased Shore A values for the tested EVA regardless of the model type ( $p < .001$ ). Higher F, EI, and UTS values were verified for the EVA with 3DT and GIV models compared to ReG and 3DnT ( $p < .001$ ). 3DnT models resulted in severe surface alteration and a greater reduction of the mechanical properties of the EVA.

**Conclusion:** The interaction of EVA with 3D resin-printed models without surface treatment or resin-reinforced Type IV dental stone models significantly affected the physical and mechanical properties of this material. The utilization of water-soluble gel coating during the post-curing process of 3D resin printed models improved the mechanical properties of the EVA, similarly when this material was plasticized over conventional Type IV dental stone model.



**KEYWORDS**

3D-printed model, dental stone model, dental trauma, ethylene-vinyl acetate, mechanical properties, mouthguard

**1 | INTRODUCTION**

The use of mouthguards (MTG) during contact sports is strongly recommended by the policy statement on Sports Dentistry of the World Dental Federation, FDI.<sup>1</sup> MTGs absorb and dissipate impact energy from physical contact during high-impact sports activity.<sup>2,3</sup> When manufactured and utilized correctly, a custom-fit MTG can reduce the stress on teeth and surrounding tissues, promoting better adaptation, retention, and comfort.<sup>4</sup>

The mechanical performance of MTGs in terms of shock absorption is affected by several factors, such as material type, manufacturing process, and thickness.<sup>5-7</sup> The athlete's adherence to MTGs and physical performance depend on these factors.<sup>7,8</sup> Intraoral impressions taken by a dentist to obtain dental stone (cast) models are the conventional flow to fabricate custom-fit MTGs.<sup>2,5,9,10</sup> Ethylene-vinyl acetate (EVA) is the most popular material utilized to manufacture custom-fit MTGs owing to its applicability as a hot-melt adhesive layer that can be easily employed with thermoforming methods to fabricate a customized device.<sup>11-13</sup> The effectiveness of MTGs is also related to the type of EVA utilized, as well as its physical and mechanical properties.<sup>2,14,15</sup> According to the American National Standards Institute, EVA must have low water absorption, adequate hardness, impact resistance, low incidence of delamination, and be biocompatible, nontoxic, and insipid.<sup>10,13</sup>

Dental models can be obtained using Types II,<sup>16</sup> III,<sup>17-19</sup> or IV,<sup>2,20</sup> dental stones with different curing times (minutes) and expansion hardening (mm). The dental stones can also be modified, presenting resin reinforcements in their composition, which can also interact with the thermo-plasticized EVA. Digital flow has been incorporated into different dentistry procedures, optimizing several processes, minimizing costs, and reducing clinical steps.<sup>21</sup> The use of a full digital flow to produce custom-fit MTGs is being established, with companies working to develop flexible 3D printable materials. The intraoral scanners allowed to utilize the digital impressions to fabricate 3D-printed models and produce custom-fit MTGs from the plasticization of EVA over these models. However, it is still uncertain if the thermoforming of EVA over 3D resin-printed models can compromise the mechanical properties and surface characteristics of the custom-fit MTGs produced with EVA.

To the best of the author's knowledge, no study has evaluated whether the interaction between the plasticized EVA with distinct materials employed for obtaining dental models can affect the performance of resulting MTGs. Therefore, this study attempted to evaluate the effect of the contact between different materials utilized for conventional (dental stone) or 3D-printed (resin) models on the physical and mechanical properties of the EVA utilized to make custom-fit MTGs. The null hypothesis was that the mechanical

properties and surface characteristics of the EVA would not be affected by the model type employed to perform the plasticization.

**2 | MATERIALS AND METHODS**

Soft circular colored EVA sheets with 3-mm thickness and 15-mm diameter (Bioart Dental Equipment) were utilized to produce experimental specimens. The thickness (mm) of the EVA sheets was measured using a digital caliper (Mitutoyo) before and after the plasticization process (initial and final thickness).

The EVA hardness was measured using Shore A equipment (Model CV06-113, CV Instruments Europe BV), applying a perpendicular force of 10N for 10s on the EVA specimens at four locations before and after plasticization, at the contact (internal) and opposite (external) surfaces with the model (Figure 1A). Four models obtained with different materials were utilized to plasticize the EVA specimens according to the experimental groups below ( $n=30$ ).

1) 3DnT model: 3D-printed resin obtained without surface treatment (Figure 1E). The workflow software (Meshmixer 2017, Autodesk) was utilized to generate the plate model's stereolithography (STL) file. The STL files were imported into a 3D printing preprocessing software (ChiTuBox, V1.9.0). The model was positioned at the center of the platform area, and the printed supports were fabricated. The printing settings were defined: layer height of .05 mm, bottom layer count of 8, exposure time of 1.5 s, and bottom exposure time of 60 s.<sup>22</sup> An ultraviolet-sensitive (light cured at 405 nm), 3D print resin was utilized (Basic Grey, Anycubic) on a 3D printer (Anycubic Photon Mono X, Anycubic) to build the models (Figure 1B). The washing process was carried out for 15 s, and the post-cure process for 20 min using a post-curing/wash machine (Cure 2.0, Anycubic).

2) 3DT model: 3D-printed resin obtained similarly to the 3DnT model, with additional surface treatment coating (Figure 1F). The washing process was carried out for 15 s. During the post-curing process, a water-soluble transparent gel coating (KY Jelly Lubricant, Johnson & Johnson), was applied in a layer approximately 3 mm thick to cover the entire surface of the model (Figure 1C), and the light exposure post-cure process was then performed for 20 min using a post-curing/wash machine (Figure 1D).

3) GIV model: conventional Type IV dental stone model (Figure 1G). A 75×70 mm rectangular metal matrix with two central holes of 5 mm in diameter was adopted as the template for obtaining the simulated model types.<sup>13</sup> An impression of the metal model was made with alginate (Hydrogum 5, Zhermack). The impression was cast with Type IV conventional dental stone (Elite Rock, Zhermack). The water/powder ratio was set according to manufacturer's instructions, and hand mixing was carried out for up to 1 min.

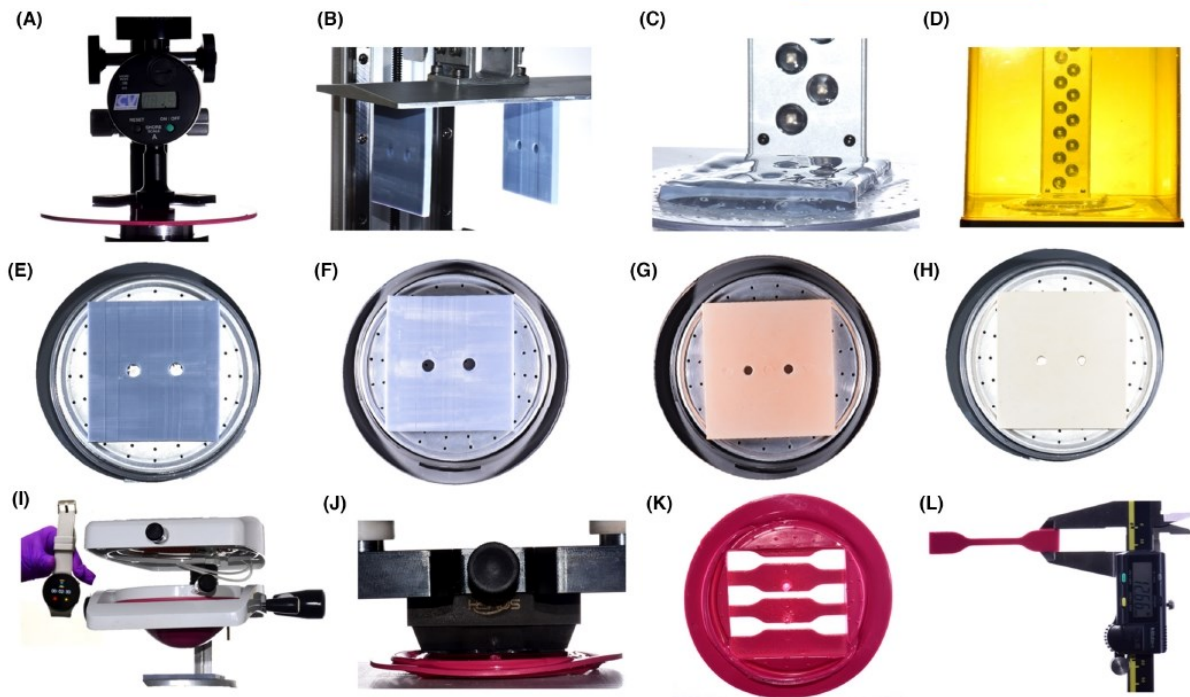


**FIGURE 1** Specimen fabrication: (A) Shore A measurement before plasticization; (B) 3D printing of models with resin; (C) Water-soluble transparent gel covering 3D-printed resin model surface; (D) Post-curing process in curing/wash machine of 3D-printed resin model with treated surface; (E) 3DnT model; (F) 3DT model; (G) GIV model; (H) ReG model; (I) EVA plate heating for 2.5 min; (J) EVA plate vacuum for 15 s; (K) Dumbbell cut of EVA sheets; (L) Aspect of three dumbbell specimens obtained for each EVA sheet; (M) Final aspect of dumbbell specimen being measured using digital caliper.

4) ReG model: resin-reinforced Type IV dental stone model (Figure 1H). The alginate impression was obtained similarly to the GIV model and cast with Type IV resin-reinforced stone (Zero Stone, Dentona). Water/powder ratio was also set according to manufacturer's instructions, and hand mixing was performed up to 1 min.

The EVA plasticization over the models was performed using a vacuum-forming (PlastiVac P7, Bio-Art), and the temperature of plasticization was recorded at 150 s (Figure 1) using an infrared thermometer (MT 395A, Minipa) at the center of the of heated surface side of the EVA sheet when placed on the heating holder of the vacuum forming machine, and also on the contact side of the sheet with the model. All specimens were prepared under vacuum for 20 s according to the manufacturer's recommendation. The EVA plate was allowed to cool for 15 min at room temperature (22°C), and then separated from the models. After EVA plasticization, the specimens were trimmed using a certified manual pressure cutting machine (SOMEH Projects Products and Services) (Figure 1J), using blade-producing dumbbell specimens according to ISO 37-2017 standard (Figure 1K). The dimensions of all specimens were checked with a digital caliper (Mitutoyo) (Figure 1L).

Macro-photography of the specimens was taken with a digital macro lens camera (DXM-I200; Nikon) for visual analyses of surface characteristics after plasticization (Figure 2). For the scanning

electron microscopy (SEM) analysis of the EVA, specimens were cut in dimensions of 10×10 mm, cleaned in an ultrasonic bath, dried, and gold-sputtered (QR 150ES, Quorum). The surface was analyzed using SEM equipment (VEGA 3 LMU, Tescan) with 20× and 100× magnifications. The patterns of alterations in the contact surface with the model were defined in four scores: (1) no alteration, (2) minimal alteration, (3) moderate alteration, and (4) severe alteration.

For mechanical analysis of the specimens, the dumbbell-shaped EVA were clamped in two grips in a universal testing machine (EMIC DL 3000, Instron) and subjected to a tensile strength test at a speed of 50 mm/min until rupture. The maximum displacement (mm) and maximum rupture force (N) were recorded using the TESC-EMIC software. The ultimate tensile strength (MPa) was calculated by dividing the rupture force (N) by the specimen cross-section area (mm<sup>2</sup>). After testing, the failure mode was classified by visual analysis according to the following levels: (I) rupture in the middle area; (II) rupture in the body; (III) rupture in the subsection area.

The rupture area (mm<sup>2</sup>), maximum force at rupture (N), maximum elongation (mm), ultimate tensile strength (MPa), EVA thickness (mm), and Shore A hardness data were tested for normal distribution (Shapiro-Wilk) and equality of variances (Levene's test). The data were then analyzed by one-way analysis of variance (ANOVA)

1600967, 0, Downloaded from <http://onlinelibrary.wiley.com/doi/10.1111/dtr.12912> by University Federal De Uberlândia, Wiley Online Library on [25/09/2024]. See the Terms and Conditions (<http://onlinelibrary.wiley.com/terms-and-conditions>) on Wiley Online Library for rules of use; OA articles are governed by the applicable Creative Commons License



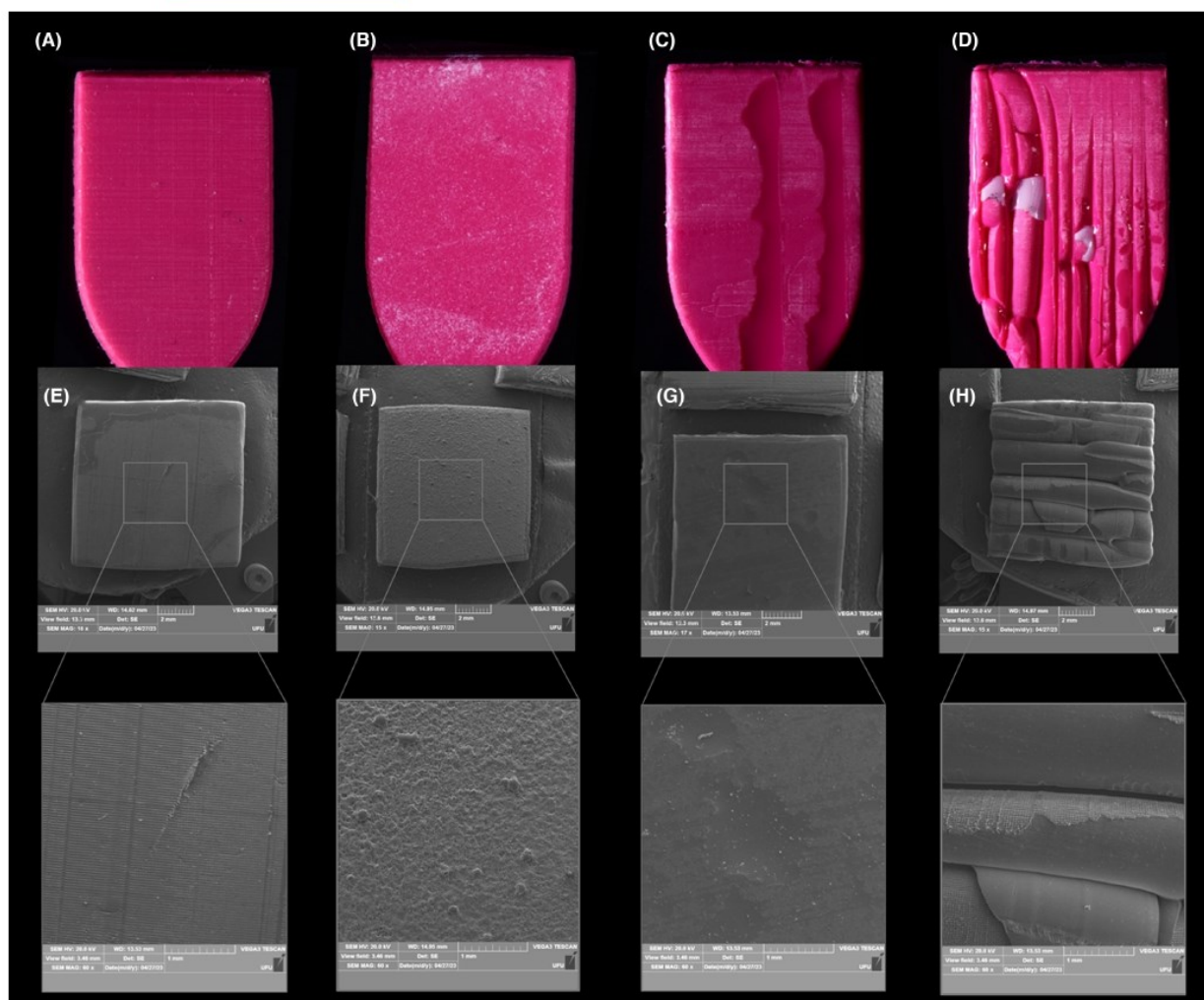


**FIGURE 2** Macro-photography and SEM images: (A) 3DT specimen, showing no EVA surface alteration; (B) GIV specimen, demonstrating negligible alteration in EVA brightness owing to the deposition of dental stone residues; (C) ReG specimen, showing irregular topography and presence of no-deep depressions; (D) 3DnT specimen, showing severe morphology alterations with irregular surface, characterized by traces of printed resin; (E) SEM image of 3DT specimen, showing regular surface with resin impression lines on EVA surface; (F) SEM image of GIV specimen, showing limited roughness on EVA surface; (G) SEM image of ReG specimen, showing no-deep depressions; (H) SEM image of 3DnT specimen, showing severe morphology alterations on EVA surface.

with repeated measures followed by Tukey's test. Failure modes were analyzed using chi-squared test. All tests employed an  $\alpha = .05$  significance level. All analyses were carried out with the statistical package Sigma Plot version 13.1. The SEM images of the specimens were analyzed qualitatively.

### 3 | RESULTS

The initial and final thickness (mm) of the specimens and the temperature ( $^{\circ}\text{C}$ ) of the EVA plasticization for all groups are presented in Table 1. One-way ANOVA showed no significant difference among the temperatures required for plasticizing EVA in the four groups tested ( $p = .301$ ). One-way ANOVA with repeated measures showed

a significant effect for the moment of the thickness measurement ( $p < .001$ ); however, no significant effect was observed for the factor model type ( $p = .441$ ). The EVA thickness reduced significantly after plasticization from 3.1 mm each to a final thickness of 2.1 mm, irrespective of the model type (Table 1). All models resulted in a similar final thickness of the EVA specimens.

The mean Shore A values and standard deviation are shown in Table 2. One-way ANOVA with repeated measures showed a significant effect for model type ( $p < .001$ ), moment of measurement ( $p < .001$ ), and also for the interaction between the model type and moment of measurement factors ( $p < .001$ ). The Shore A hardness values of EVA before and after plasticization were similar for GIV, ReG, and 3DT groups, irrespective of the tested surfaces (internal or external) ( $p = .321$ ). The 3DnT group showed

**TABLE 1** Temperature of thermo-plasticization and thickness mean and standard deviation values for EVA plates before and after thermo-plasticization.

Models	Temperature (°C)	Initial thickness (mm)	Final thickness (mm)
3D-printed resin-hydrosoluble gel	160.3 ± 7.3 A	3.1 ± 0.2 Aa	2.2 ± 0.2 Ab
3D-printed resin-no treatment	163.4 ± 8.8 A	3.0 ± 0.3 Aa	2.0 ± 0.4 Ab
Type IV gypsum	160.6 ± 8.3 A	3.1 ± 0.1 Aa	2.1 ± 0.3 Ab
Type IV resinous gypsum	163.8 ± 5.3 A	3.1 ± 0.2 Aa	2.1 ± 0.4 Ab

Note: Different letters mean significant difference among tested groups; capital letters used for comparing model type and lower case letters used for compare moment of thickness measurement.

**TABLE 2** Shore A mean and standard deviation values for EVA plates before and after thermo-plasticization measured at contact and non-contact surface of model.

Models	Initial	Noncontact surface	Contact surface
3D-printed resin-hydrosoluble gel	80.9 ± 0.3 Aa	79.1 ± 1.6 Aa	78.8 ± 0.8 Aa
3D-printed resin-no treatment	81.1 ± 0.4 Aa	75.3 ± 3.6 Bb	72.5 ± 4.9 Bc
Type IV gypsum	80.9 ± 0.5 Aa	78.9 ± 1.9 Aa	78.8 ± 1.8 Aa
Type IV resinous gypsum	81.0 ± 0.8 Aa	77.0 ± 3.1 Aa	77.3 ± 2.3 Aa

Note: Different letters mean significant difference among tested groups; capital letters used for comparing model type and lower case letters used for compare surface of EVA and compare the moment of Shore A measurement.

**TABLE 3** Rupture area, force, elongation and ultimate tensile strength after thermo-plasticization.

Models	Rupture area (mm <sup>2</sup> )	Force (N)	Elongation (%)	Ultimate tensile strength (MPa)
3D-printed resin-hydrosoluble gel	5.2 ± 1.4 A	130.4 ± 24.9 A	365 ± 32 A	25.7 ± 3.6 A
3D-printed resin-no treatment	5.0 ± 1.4 A	103.5 ± 29.2 C	315 ± 41 B	20.9 ± 4.4 C
Type IV gypsum	5.1 ± 1.0 A	125.5 ± 15.3 A	369 ± 34 A	25.1 ± 3.3 A
Type IV resinous gypsum	5.2 ± 1.3 A	116.6 ± 27.7 B	367 ± 36 A	22.3 ± 4.3 B

Note: Different letters mean significant difference among tested groups.

a significant reduction in the Shore A hardness of EVA after plasticization, mainly when measured in the contact surface with the model (internal surface) ( $p < .001$ ).

The rupture area (mm<sup>2</sup>), maximum force at rupture (N), elongation (mm), and ultimate tensile strength (MPa) of the EVA after plasticization are shown in Table 3. One-way ANOVA showed no significant differences for the rupture area of EVA among tested groups ( $p = .325$ ). One-way ANOVA showed a significant effect of the model type on EVA maximum rupture force ( $p < .001$ ). The GIV and 3DT groups had the highest and 3DnT the lowest maximum rupture force values. One-way ANOVA showed a significant effect of the model type on EVA elongation ( $p < .001$ ). The 3DnT had significantly lower elongation than all other groups. One-way ANOVA exhibited a significant effect of the model type on EVA ultimate tensile strength ( $p < .001$ ). The GIV and 3DT groups had the highest and 3DnT the lowest ultimate tensile strength.

The failure mode distribution for the specimens according to the different model types is shown in Table 4. The most frequent failure mode was located at the constricted area of the specimens, regardless of the model type employed. Chi-Square test exhibited no significant difference among failure mode distributions ( $p = .168$ ).

**TABLE 4** Rupture pattern after tensile strength test.

Models	I	II	III
3D-printed resin-hydrosoluble gel	14	16	0
3D-printed resin-no treatment	9	21	0
Type IV gypsum	16	14	0
Type IV resinous gypsum	14	16	0

Note: Chi-Squared test showed no significant difference ( $p = .168$ ).

Representative macrophotography and SEM images of the EVA surfaces for all tested groups are shown in Figure 2. The visual analysis showed that 3DT resulted in no EVA surface changes (Figure 2A), and GIV showed a slight alteration in the EVA brightness, characterized by the deposition of dental stone residues (Figure 2B). ReG showed irregular topography and the presence of no-deep depression (Figure 2C). The internal EVA surface in contact with 3DnT resulted in severe morphology alteration with an irregular surface, characterized by traces of printed resin impregnated on the EVA (Figure 2D). The SEM image of the 3DT group showed a regular surface with the resin impression lines represented on the



EVA (Figure 2E). The GIV showed small roughness on the EVA surface (Figure 2F), and the EVA in contact with ReG confirmed the presence of little no-deep depressions (Figure 2G). SEM image of the 3DnT group confirmed the severe morphology alterations on the EVA surface (Figure 2H).

#### 4 | DISCUSSION

The analysis of the surface alterations and mechanical parameters of plasticized EVA over different types of materials was able to detect the model effect during the thermoplasticization to produce custom-fit MTGs. The 3D-printed resin without surface treatment (3DnT) and resin-reinforced Type IV dental stone (ReG) models significantly reduced the physical and mechanical properties of thermoplasticized EVA; therefore, the null hypothesis was rejected.

The lack of standardization for manufacturing protocols can lead to inadequate performance of custom-fit MTGs.<sup>9,23</sup> Several factors, such as the type of material adopted,<sup>24</sup> impression technique/materials, and thickness of the MTGs, affect its effectiveness and comfort.<sup>7,25</sup> EVA is the preferable material for the fabrication of MTGs because of its plasticization properties and manipulation as a hot-melt adhesive, with shock resistance capacity and favorable biocompatibility.<sup>26</sup>

When manufacturing MTG, the heating temperature should not be lower than approximately 120°C for EVA sheets. However, if the temperature exceeds 150°C, the MTG sheets can twisted, and the formability is deteriorated.<sup>27</sup> In the present study, temperature measurement was conducted on the upper surface of the EVA sheet near the heated resistance, resulting in a higher temperature value (160°C). When a second temperature measurement was taken at the center of the plate on the side in contact with the model, an average temperature of 130°C was obtained.

EVA is a thermoplastic composed of a hydrophobic (nonpolar) rigid polyethylene backbone and a flexible hydrophilic (polar) vinyl acetate.<sup>28</sup> The heating and vacuuming involved in the manufacture of MTGs might cause orientation changes in the polymer molecules and induce residual stress on the final structure of the material.<sup>29</sup> The residual contaminants in the 3DnT and ReG model types can increase these alterations, reducing the EVA mechanical properties.

Irregular EVA surfaces, such as that observed after plasticization using the 3DnT model, can develop retention areas, such as grooves or wrinkles where the saliva or other fluids can penetrate, creating an environment for bacterial accumulation and unpleasant odors.<sup>10,30</sup> The irregular internal surface of the MTG can also cause soft tissue irritation and discomfort, making the MTG unfit for use. Maintaining a smooth surface is crucial to ensure adequate hygiene of the MTG.<sup>30,31</sup>

Custom-fit MTGs need to properly fit the teeth and soft tissues.<sup>2</sup> This is typically achieved through individualized impression(s) of the maxillary arch and production of the final cast model, which can be performed by conventional or digital techniques. The utilization of Type IV conventional dental stone showed better accuracy

than master models and a better repeatability coefficient.<sup>32</sup> The mixing method had no significant effects on the physical properties of dental stones.<sup>33</sup> The water/powder ratio is an important factor in achieving better physical properties for the hardened plaster.<sup>34</sup> The present study confirmed that the Type IV conventional dental stone remains the gold standard for manufacturing MTGs, offering good surface quality, reduced interaction with EVA material, and predictability during thermoplasticization. However, Type IV resin-reinforced dental stone led EVA specimens to a significant loss of Shore A hardness, which can result in softer and more flexible MTGs, reducing the ability of the material to absorb impacts.<sup>3</sup>

3D-printed resin models without water-soluble gel coating treatment negatively impacted the EVA specimens' mechanical properties and surface integrity. The contact of plasticized EVA, under high temperature, with untreated 3D-printed resin models resulted in the incorporation of resin residues into the EVA matrix, affecting the resulting specimens' surface heterogeneity and mechanical properties. During UV curing, oxygen in contact with 3D-printed models inhibits polymerization, resulting in an under-cured polymer.<sup>35</sup> Moreover, oxygen can also result in a highly heterogeneous structure.<sup>36</sup> This can interfere with resin polymerization, resulting in incomplete curing, deformations, or low print quality. This aspect partially explains the surface alterations observed on the EVA plasticized over 3DnT models. To avoid this, an oxygen shielding product application over the 3D-printed model to provide an oxygen-inhibition layer can be utilized during the curing process, allowing for more efficient and controlled polymerization. The surface treatment with the application of transparent water-soluble transparent gel on the 3D-printed resin model still allowed the violet light transmission, resulting in oxygen inhibition and improved polymerization. This aspect can explain the better performance of the EVA plasticized over 3DnT models and must be included in the protocol for obtaining printed models for producing custom-fit MTGs.

Considering that the diversity of the thermoforming machines for producing the MTG, it is suggested to assess whether the type of machine influences the resulting properties of MTGs. Digital workflow in dentistry has become very popular, increasing its importance in daily procedures. Digital approaches are expected to be more involved in manufacturing MTGs in the next years, owing to comfort, precision, effectiveness, and customization possibilities.<sup>37</sup> A full digital workflow for MTGs would help reduce waste by eliminating the need for the impression of physic models and facilitate the storage of patient information to fabricate novel MTGs whenever necessary.<sup>21</sup> However, it is vital to consider the proper management of the 3D printing process (for models or MTGs), particularly the disposal of resin waste generated by supports or equipment cleaning, to promote proper waste management and environmental care.

#### 5 | CONCLUSION

Within the limitations of the study design, the following conclusions can be drawn.

- The interaction of a 3D-printed resin model without surface treatment compromised the EVA's surface characteristics and mechanical properties.
- Resin-reinforced Type IV dental stone altered the surface characteristics and mechanical properties of the EVA.
- Conventional Type IV dental stone is still considered the gold standard for manufacturing MTGs owing to its reproducibility, good surface quality, and lack of negative interaction with EVA.
- Applying a water-soluble transparent gel during the post-curing of the 3D resin model eliminates the negative effect on EVA surface and mechanical properties, resulting in a similar performance to the gold standard, conventional Type IV dental stone model.

**AUTHOR CONTRIBUTIONS**

**Airin Karelys Avendaño Rondón:** Experimental development; Data Acquisition; Literature Search; Data Analysis; Manuscript Preparation and Manuscript editing. **Maribí Isomar Terán Lozada:** Experimental development; Data Acquisition; Literature Search; Data Analysis; Manuscript Preparation and Manuscript editing. **Priscilla Barbosa Ferreira Soares:** Conception and Design; Data analysis; Manuscript editing. **Luis Henrique Araújo Raposo:** Conception and Design; Manuscript Revision and Manuscript Editing. **Carlos José Soares:** Conception and Design; Literature Search; Data analysis; Funding Acquisition; Manuscript Editing and Manuscript Revision. All the authors read and approved the final manuscript.

**FUNDING INFORMATION**

This study was supported by grants from CAPES – Finance code 001 (Coordenação de Aperfeiçoamento de Pessoal de Nível Superior), National Council for Scientific and Technological Development (INCT-Saúde Oral e Odontologia, CNPq – Grants 406840/2022-9 and CNPq – Grants 422603/2021-0) and FAPEMIG (Fundação de Amparo à Pesquisa de Minas Gerais, Grants APQ-04262-2). This study was carried out at the Biomechanics, Biomaterials and Cell Biology Research Centre - CPBIO at UFU (Federal University of Uberlândia).

**CONFLICT OF INTEREST STATEMENT**

The authors confirm that they have no conflict of interest.

**DATA AVAILABILITY STATEMENT**

The data that support the findings of this study are available from the corresponding author upon reasonable request.

**ETHICS STATEMENT**

No ethic approval was required for this paper.

**ORCID**

**Airin Karelys Avendaño Rondón**  <https://orcid.org/0000-0002-3185-9622>  
**Maribí Isomar Terán Lozada**  <https://orcid.org/0000-0002-7094-4571>

**Priscilla Barbosa Ferreira Soares**  <https://orcid.org/0000-0002-4492-8957>  
**Luis Henrique Araújo Raposo**  <https://orcid.org/0000-0003-2726-9133>  
**Carlos José Soares**  <https://orcid.org/0000-0002-8830-605X>

**REFERENCES**

1. FDI World Dental Federation. FDI policy statement on sports dentistry: adopted by the FDI general assembly, September 2016, Poznan, Poland. *Int Dent J.* 2017;67:18–9.
2. Verissimo C, Costa PV, Santos-Filho PC, Tantbirojn D, Versluis A, Soares CJ. Custom-fitted EVA Mouthguards: what is the ideal thickness? A dynamic finite element impact study. *Dent Traumatol.* 2016;32:95–102.
3. Bragança GF, Vilela ABF, Soares PBF, Tantbirojn D, Versluis A, Soares CJ. Influence of ceramic veneer thickness and antagonist on impact stresses during dental trauma with and without a mouthguard assessed with finite element analysis. *Dent Traumatol.* 2021;37:215–22.
4. Kalman L, Dal Piva AMO, de Queiroz TS, Tribst JPM. Biomechanical behavior evaluation of a novel hybrid occlusal splint-mouthguard for contact sports: 3D-FEA. *Dent J.* 2021;10:3.
5. Carvalho VF, Soares PB, Verissimo C, Pessoa RS, Versluis A, Soares CJ. Mouthguard biomechanics for protecting dental implants from impact: experimental and finite element impact analysis. *Int J Oral Maxillofac Implants.* 2018;33:335–43.
6. Takahashi M, Bando Y. Fabrication method to maintain mouthguard thickness regardless of the model angle. *Dent Traumatol.* 2021;37:131–7.
7. Sun Z, Zhang J, Sun R, Zhang M, Zhong Q, Huang M, et al. Effects of different custom-made mouthguard palatal extensions on the stress-state of dentoalveolar structures: a 3D-FEA. *Clin Oral Investig.* 2023;27:3809–16.
8. Knapik JJ, Marshall SW, Lee RB, Darakjy SS, Jones SB, Mitchener TA, et al. Mouthguards in sport activities: history, physical properties and injury prevention effectiveness. *Sports Med.* 2007; 37:117–44.
9. Zamora-Olave C, Willaert E, Montero-Blesa A, Riera-Punet N, Martinez-Gomis J. Risk of orofacial injuries and mouthguard use in water polo players. *Dent Traumatol.* 2018;34:406–12.
10. Sousa AM, Pinho AC, Piedade AP. Mechanical properties of 3D printed mouthguards: influence of layer height and device thickness. *Mater Des.* 2021;203:109624.
11. Takahashi M, Bando Y. Effect of the anteroposterior position of the model on fabricated mouthguard thickness: part 2 influence of sheet thickness and material. *Dent Traumatol.* 2018;34:370–7.
12. Dal Piva AMO, Tribst JPM, Borges ALS, Kleverlaan CJ, Feilzer AJ. The ability of mouthguards to protect veneered teeth: a 3D finite element analysis. *Dent Traumatol.* 2023;39:191–9.
13. de Melo C, Resende JB, Lozada MIT, Mendoza LCL, Ribeiro MTH, Soares PBF, et al. Effect of surface treatment of ethylene vinyl acetate on the delamination of custom-fitted mouthguards. *Dent Traumatol.* 2023;39:324–32.
14. Patrick DG, van Noort R, Found MS. Scale of protection and the various types of sports mouthguard. *Br J Sports Med.* 2005; 39:278–81.
15. Parker K, Marlow B, Patel N, Gill DS. A review of mouthguards: effectiveness, types, characteristics and indications for use. *Br Dent J.* 2017;222:629–33.
16. Farrington T, Coward T, Onambele-Pearson G, Taylor RL, Earl P, Winwood K. The effect of model inclination during fabrication on mouthguard calliper-measured and CT scan-assessed thickness. *Dent Traumatol.* 2016;32:192–200.



17. Takahashi M, Bando Y. Thermoforming technique for suppressing reduction in mouthguard thickness: part 2 effect of model height and model moving distance. *Dent Traumatol.* 2020;36:543–50.
18. Dias A, Redinha L, Tavares F, Silva L, Malaquias F, Pezarat-Correira P. The effect of a controlled mandible position mouthguard on upper body strength and power in trained rugby athletes—a randomized within subject study. *Injury.* 2022;53:457–62.
19. Kalra A, Harrington C, Minhas G, Papageorgiou SN, Cobourne MT. Wearability and preference of mouthguard during sport in patients undergoing orthodontic treatment with fixed appliances: a randomized clinical trial. *Eur J Orthod.* 2022;44:101–9.
20. Flores-Figueiras C, Zamora-Olave C, Willaert E, Martinez-Gomis J. Effect of thickness and occlusal accommodation on the degree of satisfaction with mouthguard use among water polo players: a randomized crossover trial. *Dent Traumatol.* 2020;36:670–9.
21. Li Z, Wang S, Ye H, Lv L, Zhao X, Liu Y, et al. Preliminary clinical application of complete workflow of digitally designed and manufactured sports mouthguards. *Int J Prosthodont.* 2020;33:99–104.
22. de Bragança GF, de Souza IF, Soares PBF, Soares CJ. Biomechanical effects of a hard insert and air space in mouthguards on the shock absorption and protection against fractures of direct resin composite veneers from trauma. *Dent Traumatol.* 2023;39:314–23.
23. Karaganeva R, Pinner S, Tomlinson D, Burden A, Taylor R, Yates J, et al. Effect of mouthguard design on retention and potential issues arising with usability in sport. *Dent Traumatol.* 2019;35:73–9.
24. Tribst JPM, Dal Piva AMO, Kalman L. Stress concentration of hybrid occlusal splint-mouthguard during a simulated maxillofacial traumatic impact: 3D-FEA. *Dent J (Basel).* 2022;10:65.
25. Sliwkanich L, Ouanounou A. Mouthguards in dentistry: current recommendations for dentists. *Dent Traumatol.* 2021;37:661–71.
26. Trzaskowski M, Mańka-Malara K, Szczesio-Włodarczyk A, Sokołowski J, Kostrzewa-Janicka J, Mierzwińska-Nastalska E. Evaluation of mechanical properties of 3d-printed polymeric materials for possible application in mouthguards. *Polymers.* 2023;15:898.
27. Tanabe G, Churei H, Wada T, Takahashi H, Uo M, Ueno T. The influence of temperature on sheet lamination process when fabricating mouthguard on dental thermoforming machine. *J Oral Sci.* 2020;62:23–7.
28. Carmona AR, Colorado Lopera HA. A new composite made from luffa *Cylindrica* and ethylene vinyl acetate (EVA): mechanical and structural characterization for its use as Mouthguard (MG). *J Mech Behav Biomed Mater.* 2022;126:105064.
29. Meng FH, Schricker SR, Brantley WA, Mendel DA, Rashid RG, Fields HW Jr, et al. Differential scanning calorimetry (DSC) and temperature-modulated DSC study of three mouthguard materials. *Dent Mater.* 2007;23:1492–9.
30. Ribeiro YJS, Delgado RZR, Paula-Silva FWG, Rematal-Valdes B, Feres MG, Palma-Dibb RG, et al. Sports mouthguards: contamination, roughness, and chlorhexidine for disinfection—a randomized clinical trial. *Braz Dent J.* 2021;32:66–73.
31. Hayashi H, Naiki Y, Murakami M, Oishi A, Takeuchi R, Nakagawa M, et al. Effects of cleaning sports mouthguards with ethylene-vinyl acetate on oral bacteria. *PeerJ.* 2022;10:e14480.
32. Tripodi D, Cosi A, Fulco D, D'Ercole S. The impact of sport training on oral health in athletes. *Dent J.* 2021;9:51.
33. Azer SS, Kerby RE, Knobloch LA. Effect of mixing methods on the physical properties of dental stones. *J Dent.* 2008;36:736–44.
34. Phillips RW. *Skinner: materiais dentários.* 9th ed. Rio de Janeiro: Guanabara Koogan; 1993. p. 40–53.
35. Lee SY, Lim JH, Kim D, Lee DH, Kim SG, Kim JE. Evaluation of the color stability of 3D printed resin according to the oxygen inhibition effect and temperature difference in the post-polymerization process. *J Mech Behav Biomed Mater.* 2022;136:105537.
36. Huang DR, Yongxia Y, Ruoning H, Zhiguo Y. Preparation and characterization of a novel ultraviolet/thermal dual-curing thiol-ene/polyurethane acrylate coating. *J Coat Technol Res.* 2021;18:18–1116.
37. Hada T, Komagamine Y, Kanazawa M, Minakuchi S. Fabrication of sports mouthguards using a semi-digital workflow with 4D-printing technology. *J Prosthodont Res.* 2023;12. doi:10.2186/jpr.JPR\_D\_22\_00274. Epub ahead of print.

**How to cite this article:** Rondón AKA, Lozada MIT, Soares PBF, Raposo LHA, Soares CJ. Effect of different materials for conventional and 3D-printed models on the mechanical properties of ethylene-vinyl acetate utilized for fabricating custom-fit mouthguards. *Dental Traumatology.* 2023;00:1–8. <https://doi.org/10.1111/edt.12912>

## CAPÍTULO 2

### ARTIGO 2

Adaptation and biomechanical performance of custom-fit mouthguards produced using conventional and digital workflow: A comparative in-vitro study

Artigo submetido no periódico Dental Traumatology



**Adaptation and biomechanical performance of custom-fit mouthguards produced using conventional and digital workflows: a comparative in-vitro strain analysis**

Airin Karelys Avendaño Rondon<sup>1</sup>, Maribí Isomar Terán Lozada<sup>1</sup>, Izabela Batista Cordeiro<sup>1</sup>, Paulo Cesar Junqueira Bandeira<sup>1</sup>, Liran Levin<sup>2</sup>, Priscilla Barbosa Ferreira Soares<sup>3</sup>, Carlos José Soares<sup>1\*</sup>

<sup>1</sup>Department of Operative Dentistry and Dental Materials, Dental School, Federal University of Uberlândia, Uberlândia, Uberlândia, Minas Gerais, Brazil.

<sup>2</sup>Faculty of Medicine and Dentistry, University of Alberta, Edmonton, Canada.

<sup>3</sup>Department of Periodontology and Implantology, School of Dentistry, Federal University of Uberlândia, Uberlândia, Minas Gerais, Brazil.

**Running title:** Custom-fit mouthguards using digital workflow

**Keywords:** plaster model; 3D printed model; mouthguard; alginate impression; digital impression.

**Corresponding author:**

Dr. Carlos José Soares

Federal University of Uberlândia, School of Dentistry

Avenida Pará, 1720, Bloco 4L, anexo A, sala 42, Campos Umuarama.

Uberlândia, Minas Gerais, Brazil

Zip-Code: 38400-902

E-mail: carlosjsoares@ufu.br

## CONFLICT OF INTEREST STATEMENT

The authors confirm that they have no conflict of interest.

## DATA AVAILABILITY STATEMENT

The data that support the findings of this study are available from the corresponding author upon reasonable request.

## AUTHOR CONTRIBUTIONS

**Airin Karelys Avendaño Rondón:** Experimental development, Data Acquisition, Literature Search, Data Analysis, Manuscript Preparation and Manuscript editing. **Maribí Isomar Terán Lozada:** Experimental development, Data Acquisition, Literature Search, Data Analysis, Manuscript Preparation and Manuscript editing. **Izabela Batista Cordeiro:** Experimental development, Data Acquisition, Literature Search, Manuscript Preparation and Manuscript editing. **Paulo Cesar Junqueira Bandeira:** Experimental development, Data Acquisition. **Liran Levin:** Manuscript Preparation and Manuscript editing. **Priscilla Barbosa Ferreira Soares:** Conception and Design, Data analysis, Manuscript editing. **Carlos José Soares:** Conception and Design, Literature Search, Data analysis, Funding Acquisition, Manuscript Editing and Manuscript Revision.

All the authors read and approved the final manuscript.

## ORCID

Airin Karelys Avendaño Rondón: <https://orcid.org/0000-0002-3185-9622>

Maribí Isomar Terán Lozada: <https://orcid.org/0000-0002-7094-4571>

Izabela Batista Cordeiro: <https://orcid.org/0009-0002-1386-2382>

Paulo Cesar Junqueira Bandeira: <https://orcid.org/0009-0002-4393-7525>

Liran Levin: <https://orcid.org/0000-0002-8123-7936>

Priscilla Barbosa Ferreira Soares: <https://orcid.org/0000-0002-4492-8957>

Carlos José Soares: <https://orcid.org/0000-0002-8830-605X>

### **E-mails**

Airin Karelys Avendaño Rondón: [airinrondon@gmail.com](mailto:airinrondon@gmail.com)

Maribí Isomar Terán Lozada: [maribi.lozada@ufu.br](mailto:maribi.lozada@ufu.br)

[Izabela Batista Cordeiro: Izabela.cordeiro@ufu.br](mailto:Izabela.Batista.Cordeiro@ufu.br)

[Paulo Cesar Junqueira Bandeira: paulocesarpetim@hotmail.com](mailto:Paulo.Cesar.Junqueira.Bandeira@hotmail.com)

Liran Levin: [liran@ualberta.ca](mailto:liran@ualberta.ca)

Priscilla Barbosa Ferreira Soares: [pbfoares@ufu.br](mailto:pbfoares@ufu.br)

Carlos José Soares: [carlosjsoares@ufu.br](mailto:carlosjsoares@ufu.br)

## Adaptation and biomechanical performance of custom-fit mouthguards produced using conventional and digital workflows: a comparative in-vitro strain analysis

### ABSTRACT

**Background/Objectives:** The use of different models for the fabrication of custom-fit mouthguards (MTGs) can affect their final thickness, adaptation, and shock-absorption properties. This study aimed to evaluate the adaptation, thickness, and shock absorption of ethylene-vinyl acetate (EVA) thermoplastic MTGs produced using conventional plaster or three-dimensional (3D) printed models.

**Materials and Methods:** A typical model with simulated soft gum tissue was used as the reference model to produce MTGs with the following two different protocols: plast-MTG using a conventional impression and plaster model (n = 10) and 3DPr-MTG using a digital scanning and 3D printed model (n = 10). A custom-fit MTG was fabricated using EVA sheets (Bioart) plasticized over different models. The MTG thickness (mm), internal adaptation (mm) to the typodontic model, and voids in the area (mm<sup>2</sup>) between the two EVA layers were measured using cone-beam computed tomography images and Mimics software (Materialize). The shock absorption of the MTG was measured using a strain-gauge test with a pendulum impact at 30° with a steel ball over the typodont model with and without MTGs. Data were analyzed using one-way analysis of variance with repeated measurements, followed by Tukey's post hoc tests.

**Results:** The 3DPr-MTG showed better adaptation than that of the Plast-MTG at the incisal/occlusal and lingual tooth surfaces (p < 0.001). The 3DPr-MTG showed a thickness similar to that of the Plast-MTG, irrespective of the measured location. MTGs produced

using both model types significantly reduced the strain values during horizontal impact (3DPr-MTG 86.2% and Plast-MTG 87.0%) compared with the control group without MTG ( $p < 0.001$ ).

**Conclusion:** The MTGs showed the required standards regarding thickness, adaptation, and biomechanical performance, suggesting that the number and volume of voids had no significant impact on their functionality. 3D printed models are a viable alternative for MTG production, providing better adaptation than the Plast-MTG at the incisal/occlusal and lingual tooth surfaces and similar performance as the MTG produced with the conventional protocol.

**Keywords:** 3D-printed model; dental stone model; dental trauma; ethylene vinyl acetate; mechanical properties.

## 1. INTRODUCTION

Mouthguards (MTG) can absorb impacts and reduce stress and strain transmitted to the teeth because of trauma during sports activities.<sup>1-4</sup> Use of MTGs decreases the possibility of tooth fracture and damage to the adjacent tooth structures,<sup>5</sup> mandibular condyle, and articular disc.<sup>6,7</sup>

The impact absorption of custom-fit MTGs is affected by several factors, such as MTG type,<sup>8,9</sup> manufacturing process,<sup>10</sup> and the presence of antagonist contacts.<sup>2,11</sup> Among the different MTG types, custom-fit MTGs provide superior performance in terms of comfort, fit, stability, respiratory capacity, phonetics, and protection of dental structures.<sup>12-14</sup> Although these factors influence MTG performance, thickness is the most

important parameter for shock absorption.<sup>15-17</sup> The shock absorption ability can be improved by increasing the thickness of the MTGs. However, the ideal thickness is limited to approximately 4.0 mm,<sup>15,16</sup> as thicker MTGs might be related to poor athletic performance, reduced respiratory efficiency, and comfort issues.<sup>18</sup>

The effect of the model position on the forming table,<sup>19</sup> angle of the model, and thermoforming method can influence the thickness of the MTGs.<sup>19</sup> The shape of the model is one of the main factors affecting the thickness of custom-fit MTGs. A model with an acute angle can prevent thinning of the MTG, even if the anterior height of the model is increased.<sup>20</sup>

The adaptation and stability of the MTGs can also contribute to mechanical performance.<sup>11,21,22</sup> Custom-fit MTGs offer better adaptation than mouth-formed and prefabricated MTGs.<sup>8,22</sup> The MTG should properly fit and accurately adapt to the maxillary arch to provide adequate protection and avoid dislodgement on impact.<sup>23,24</sup> MTGs are fabricated using dental impressions creating individualized adaptation to the patient.<sup>25</sup> Clinically, during the MTGs fabrication, plaster models are mounted on an adjustable articulator that replicates mandibular movements and then adjusted according to the occlusion and maximum intercuspal position.<sup>25,26</sup>

The use of three-dimensional (3D) printed resin models to fabricate the thermoplastic ethylene-vinyl acetate (EVA) MTGs has emerged as an innovative and promising area in the field of dentistry.<sup>27</sup> The applications of 3D printing in the medical and dental fields have garnered significant attention in recent years.<sup>28</sup> In dentistry, this technology provides numerous benefits, including increased efficiency, easy customization of dental appliances and products, highly accurate results.<sup>29,30</sup> At the same

way, it is possible to promoting less discomfort for patients sensitive to taste, nausea, and breathing difficulty,<sup>31</sup> and eliminates all fabricating errors encountered by conventional methods, such as the distortion of impression material.<sup>32</sup>

Therefore, the aim of this study was to evaluate the adaptation, thickness, and mechanical performance of custom-fit MTGs fabricated using a conventional protocol or digital workflow with 3D-printed models. The null hypothesis was that the adaptation, thickness, and shock absorption of the MTGs would not be affected by the model used for plasticization.

## 2. MATERIALS AND METHODS

A full maxillary typodont model with simulated soft gum tissue (Oclusal Prod. Odont. Ltda São Paulo, Brazil) was used as a reference to produce the following two models (Figure 1):

**1) *Plaster model (Plast-MTG)*** (n = 10): Wax was molded around the periphery of a standard impression tray (Figure 1A), and the impression of the typodont model was made using alginate (Hydrogum V, Zhermack, Italy) (Figure 1B). The materials were prepared according to the manufacturer's recommendations. The powder was extracted from the packaging using a measuring spoon. For each spoon full of powder, a one-third measure of water sample was added to the mixing bowl and mixed by automatic mixing (Oubo Algimax II GX300, Zhejiang, China) until the consistency and color were homogenous. The impression was cast with type IV dental stone (Elite Rock, Zhermack, Italy) using a plaster vibrator (VH Equipamentos, Curitiba, Brazil) (Figure 1C). The powder/water ratio was determined according to the manufacturer's instructions. The

shape and design of the plaster model were standardized according to the following parameters: the angle of the model formed between the labial surface of the central incisor and the base of the working model was defined as 90°, a height of 25 mm at the incisal edge of the maxillary central incisor, and a height of 20 mm at the mesio-buccal cusp of the maxillary first molar. The palatal extension of the model was 25 mm at the incisal edge of the maxillary first molar (Figure 1D).

**2) 3D resin printed model (3DPr-MTG) (n = 10):** The typodont model was scanned using a 3D intraoral scanner (Straumann, Virtuo Vivo, Basel, Switzerland) (Figure 1E). Stereolithography (STL) files were imported into workflow software (Meshmixer 2017, Autodesk, San Francisco, United States) to standardize the model (Figure 1F). The files in OBJ format were imported into 3D printing preprocessing software (ChiTuBox, V1.9.0, Shenzhen, China). The model was positioned at the center of the platform area and printed supports were created. The printing settings were as follows: layer height 0.05 mm, bottom layer count 6, exposure time 1.5 s, and bottom exposure time 40 s. An ultraviolet-sensitive (light-cured at 405 nm) 3D printing resin (Basic Grey, Anycubic) was used on a 3D printer (Anycubic Photon Mono X, Anycubic, Shenzhen, China) to fabricate 3D resin-printed models (Figure 1E). The washing process was conducted for 5 min. During the post-curing process, a water-soluble transparent gel coating (KY Jelly Lubricant, Johnson & Johnson, New Jersey, United States) was applied for 10 min to cover the entire surface of the model with a thickness of 3 mm using a post-curing/wash machine.<sup>27</sup> The shape and design of the printed model were the same as those of the plaster model (Figure 1F).



The MTGs were produced using two soft circular EVA sheets with a thickness of 3 mm and diameter of 15 mm (Bioart Dental Equipment, São Carlos, SP, Brazil) to obtain specimens with a final thickness of 4 mm (n = 10) (Figure 2A). The first EVA plate was heated in a vacuum plasticizer (PlastiVac P7, Bio-Art) for 150 s and then prepared by vacuum forming for 20 s following the manufacturer's recommendations. It was allowed to cool for 15 min at room temperature (22 °C) (Figure 2B). The first layer of the MTG was cut at the bottom of the vestibular groove, and a 5-mm palatal extension was performed using a N° 15 scalpel (Figure 2C), with finishing and polishing of the edge performed with a Maxicut De Zirconia bur (Figure 2D) and Scotch Brite brushes using a low-speed handpiece (Figure 2E). The resin monomer (VIPI Flash, VIPI Odonto Products, Pirassununga, Brazil) (Figure 2F) was applied to the outer surface of the first EVA plate and inner surface of the second EVA plate (Figure 2G) for 1 min. Air spray was then applied to the plate surface for 10 s as the final treatment.<sup>10</sup> The second plate was plasticized for 150 s and bonded over the first EVA plate and stored at room temperature (22 °C) (Figure 2H), thereby obtaining an MTG of 4.0 mm in thickness.

To measure the MTG thickness, internal adaptation to the typodont model, and presence of voids between the two EVA layers, cone-beam computed tomographic scanning (i-CAT GXCB-500; Imaging Sciences International, Hatfield, USA), was used with voxel dimensions of 0.125 mm for each mouthguard on the reference model. A total of 704 sections were obtained with 23 s of acquisition and exposure parameters of 120 kV and 3.0–7.0 mA. The DICOM files were exported and analyzed using Mimics software (Materialize Dental, Leuven, Belgium). The files were used to measure the thickness (mm) of the MTGs (Figure 3), adaptation expressed by the distance (mm) between the external surface of the typodont model and the internal surface of the MTGs (Figure 4), and area

(mm<sup>2</sup>) of the voids present between the two EVA layers of the MTGs at six different locations: both first molars, first premolars, and central incisors, and at three different surfaces: occlusal/incisal, buccal, and lingual (Figure 5).

A unidirectional strain gauge (PA-06- 040AB- 120- LEN, Excel Sensors, São Paulo, Brazil) with a unidirectional electrical internal resistance of 120  $\Omega$  and grid size of 1 mm<sup>2</sup> was attached to the palatal surface of the upper central incisor of the typodont using a cyanoacrylate resin adhesive (Super Bonder, Loctite, SP, Brazil) (Figure 6A). The typodont model was fixed to a modified Charpy impact tester to prevent displacement during impact testing. A pendulum device with a steel ball with 227.0 g and 35.0 mm diameter was positioned on the center of the labial surface of the left central incisor from a 30-degree angle without MTG (Figure 6B) and with MTG (Figure 6C). Following previous studies,<sup>1-3</sup> the strain gauges were oriented parallel to the long axis of the tooth and parallel to the steel ball that generates the impact. This allowed for precise readings of the deformation peaks analyzed. The impact was targeted at the center of the tooth at the strain gauge level (Figure 6D). A control specimen with a strain gauge that was not subjected to impact was used to compensate for vibration and temperature variations. Both the strain gauges were connected to a half-bridge Wheatstone circuit. Data were acquired at 500 Hz and recorded using a signal transformation and data analysis software (AQDADOS 7.02, AQANALISYS, Lynx, Brazil). Shock absorption (%) was calculated from the peak strain values using a non-mouth guard control group as a reference.

The MTG thickness (mm), internal adaptation (mm), void area inside the MTGs (mm<sup>2</sup>), strain ( $\mu$ S), and shock absorption (%) were first analyzed for normal distribution (Shapiro–Wilk test) and homoscedasticity (Levene's test). One-way analysis of variance

was performed for strain ( $\mu\text{S}$ ) and shock absorption (%). One-way analysis of variance with repeated measurements was performed for MTG thickness (mm), internal adaptation (mm), and void area inside the MTGs ( $\text{mm}^2$ ), followed by Tukey's post-hoc tests. All tests used an  $\alpha = 0.05$ , and all analyses were performed using the statistical package Sigma Plot version 13.1 (Systat Software).

### 3. RESULTS

The mean thicknesses (mm) and standard deviations of the MTGs at different locations are shown in Figure 7. Plasticization significantly reduced the thickness of all the MTGs. The 3DPr-MTG showed a thickness similar to that of the Plas-MTG, irrespective of the location ( $p = 0.371$ ). Both MTGs had greater thicknesses at the premolars and molars than at the incisors for the buccal alveolar, buccal tooth, and incisal/occlusal surfaces ( $p < 0.001$ ). However, in the lingual area, the incisors had greater thicknesses than the premolars and molars ( $p < 0.001$ ), and in the lingual alveolar area, the incisors and premolars had greater thicknesses than the molars ( $p < 0.001$ ). The greatest thicknesses were observed on the occlusal surfaces of the premolars and molars.

The mean adaptation (mm) and standard deviation of the MTGs at different locations are shown in Figure 8. The 3DPr-MTG showed better adaptation than the Plas-MTG at the incisal/occlusal and lingual tooth surfaces ( $p < 0.001$ ), and was similar at all other surfaces. Adaptation was significantly worse in the occlusal and lingual alveolar locations ( $p < 0.001$ ). The buccal surfaces and incisors tended to show better adaptation.

The mean void area ( $\text{mm}^2$ ) and standard deviation of the MTGs at different locations are shown in Figure 9. The 3DPr-MTG showed the lowest void area at the lingual

and buccal locations ( $p < 0.001$ ), which was similar at all other locations. The void area was significantly larger in the lingual region ( $p < 0.001$ ).

The mean of the strain peak ( $\mu\text{S}$ ) and standard deviations of the horizontal impact at  $30^\circ$  in the pendulum device are shown in Figure 10. One-way ANOVA showed that MTGs fabricated using both model types significantly reduced the strain values during horizontal impact compared with the control group without MTG ( $p < .001$ ). The 3DPr-MTG and Plas-MTG had similar strains ( $P = 0.256$ ). The percentage of shock absorption for each type of MTG is shown in Figure 10. The 3DPr-MTG demonstrated shock absorption similar to that of Plas-MTG (86.2% and 87.0%, respectively, compared with the values obtained for the control group without MTG). The failure mode frequencies recorded by the macrophotograph analysis are listed in Table 1. The chi-square test showed that the no-MTG group had a significantly higher severity of failure mode distribution than both MTG groups ( $p < .001$ ). None of the 3DPr-MTG or Plast-MTG specimens exhibited fractures (Type I failure mode). However, the no-MTG group had one specimen with a root fracture (Type IV) (Figure 6E) and four specimens with fractures of the lingual alveolar bone (Type III).

#### **4. DISCUSSION**

The analysis of the adaptation, thickness, and shock absorption of the custom-fit MTGs demonstrated that the type of model used for MTG fabrication had no significant influence on the MTG thickness and biomechanical performance. However, the 3DPr-MTG showed better adaptation than the Plast-MTG at the incisal/occlusal and lingual tooth surfaces. Therefore, the null hypothesis was rejected.

The assessment of MTG displacement is a crucial parameter for impact absorption, as it must remain in the correct position to function properly.<sup>16</sup> This is crucial to prevent injuries resulting from dental trauma, such as tooth fracture,<sup>2</sup> damage to adjacent structures, to the mandibular condyle, and the articular disc.<sup>11</sup> It can also prevent the stress concentration on the permanent tooth germ in the case of the trauma occurred on deciduous teeth.

The adaptation of the MTG to the soft tissue, proximal area, and dental surfaces has been evaluated in previous studies using a model with silicone test material on an articulator,<sup>33</sup> as well as directly in the oral cavity.<sup>34</sup> In this study, the use of CBCT helped not only to evaluate the adaptation of the model but also to check the presence of voids between the two layers of EVA for the MTGs. This method offers a detailed visualization of the internal surface of the MTG and its adaptation to oral structures, allowing information to optimize the MTG design and performance during impact absorption.

The MTG thickness is a critical factor affecting the mechanical performance and shock absorption capacity of mouthguards. It is widely recognized that MTG thickness decreases after vacuum forming.<sup>21</sup> The MTG thickness reduction is influenced by various factors, including sheet material, forming methods, heating temperature,<sup>35</sup> and the design of the plaster model.<sup>35,36</sup> Thicknesses of 3–4 mm are typically recommended for custom-fitted MTG.<sup>16</sup> Thus, this study found MTG thickness values similar to the recommended values irrespective of the model type used.

Although adaptation is an important factor for MTG comfort and effectiveness, the results indicate that even with small variations in MTG adaptation, consistent and effective biomechanical performance in protecting against orofacial injuries can be

ensured.<sup>25</sup> This may be attributed to the quality of the EVA material used, which possesses an ideal elastic modulus for MTG fabrication.<sup>37</sup>

The occurrence of void in the EVA thermoforming process was likely due to the anatomy of the model, where a larger space, primarily around the posterior teeth, reduced the vacuum's effectiveness. However, despite the presence of the voids between the EVA layers, no significant effect was observed on the biomechanical performance of the tested MTGs. The presence of these minimal spaces was probably caused by the surface treatment of the EVA.<sup>10</sup>

The adhesion is primarily influenced by the surface energy of the EVA. A reduction in the interfacial tension or interfacial energy results in stronger attractive forces and interactions between different materials.<sup>38</sup> Additionally, lower contact angles are associated with better bonding interaction.<sup>39</sup> The use of acrylic resin monomer reduced the contact angle, creating a more reactive EVA surface than in the other groups.<sup>10</sup> All of which can explain the minimal occurrence of voids between the EVA layers.

The MTGs met the required standards regarding thickness, adaptation, and biomechanical performance, suggesting that the number and volume of voids had no significant impact on their functionality. This finding highlights the robustness of the manufacturing process and its ability to produce high-quality MTGs.

The use of the typodont model to assess the impact of MTGs proved to be an effective and reliable strategy in previous studies and in the present work.<sup>40</sup> Because of the difficulty in obtaining more realistic models that adequately represent dental anatomy and the biomechanical properties of oral tissues, the use of the typodont model is an adequate and practical alternative.<sup>41</sup> Although different experimental setups using metal

or printed resin models have been employed to test MTGs,<sup>3,42</sup> it is important to note that all these models exhibit significant differences in the elastic modulus of dental enamel, dentin, and bone tissues,<sup>3</sup> consequently being a limitation of this study. The absence of the periodontal ligament simulation can be also considered as a limitation of this study. In future studies, the inclusion of a more accurate simulation of the periodontal ligament could enhance the precision of the results and provide a more comprehensive understanding of the biomechanical performance of MTGs.

This study showed tooth failure modes similar to those in previous studies and also similar to the clinical condition of anterior traumatized teeth.<sup>1,15,42</sup> Such fractures involve the root dentin and pulp and are often associated with periodontal ligament and alveolar bone damage.<sup>42</sup> Their incidence in the permanent dentition is estimated to be between 0.5% and 7%, with the anterior region of the maxilla, especially the central incisors, being the most affected area.<sup>42</sup> When an impact force is applied to the human body, two possibilities can occur: if the energy is not sufficient to cause damage, then it is dissipated as thermal energy by the body.<sup>42</sup> However, if the energy is significantly higher than that can be supported by the tooth structure, it is transformed into destructive energy that can cause damage to the soft tissues, displacement, and fractures involving teeth and bone structures.<sup>43</sup>

The presence of the MTGs is effective in reducing the deformations resulting from impacts, highlighting its important protective function during sports activities.<sup>1</sup> The pendulum device used in this study was designed similarly to the conventional Charpy impact test and has been used in previous research.<sup>1,2</sup> However, this device does not simulate the moment during impact, which may limit the accurate representation of real

dental trauma situations. Additionally, frontal impact was conducted following the principle of energy conservation using a 30° angle corresponding to 1.0 m/s, which may not correspond to many other dental trauma situations.<sup>1,3</sup>

In conclusion, the possibility of using 3D-printed models to produce MTGs was explored, with promising results. The MTGs manufactured using 3D-printed models showed superior adaptation at specific tooth locations compared with mouthguards made with conventional plaster models, while maintaining similar thickness in all measured areas. Additionally, both types of MTGs significantly reduced the deformation values during horizontal impact when compared with the control group without MTG. These results suggest that 3D-printed models may be a viable alternative for MTG production, providing adaptation and performance similar to the current standard fabrication protocols.



## 5. REFERENCES

1. Verissimo C, Costa PV, Santos-Filho PC, Fernandes-Neto AJ, Tantbirojn D, Versluis A, Soares CJ. Evaluation of a dentoalveolar model for testing mouthguards: stress and strain analyses. *Dent Traumatol.* 2016;32:4-13. doi: 10.1111/edt.12197.
2. Bragança GF, Vilela ABF, Soares PBF, Tantbirojn D, Versluis A, Soares CJ. Influence of ceramic veneer thickness and antagonist on impact stresses during dental trauma with and without a mouthguard assessed with finite element analysis. *Dent Traumatol.* 2021;37:215-22. doi: 10.1111/edt.12631.
3. Bragança GF, de Souza IF, Soares PBF, Soares CJ. Biomechanical effects of a hard insert and air space in mouthguards on the shock absorption and protection against fractures of direct resin composite veneers from trauma. *Dent Traumatol.* 2023;39:314-23. doi: 10.1111/edt.12842.
4. Dal Piva AMO, Tribst JPM, Borges ALS, Kleverlaan CJ, Feilzer AJ. The ability of mouthguards to protect veneered teeth: A 3D finite element analysis. *Dent Traumatol.* 2023;39:191-9. doi: 10.1111/edt.12812.
5. Vilela ABF, Soares PBF, Almeida GA, Veríssimo C, Rodrigues MP, Versluis A, Soares CJ. Three-dimensional finite element stress analysis of teeth adjacent to a traumatized incisor. *Dent Traumatol.* 2019;35:128-34. doi: 10.1111/edt.12453.
6. Fernandes LM, Neto JCL, Lima TFR, Magno MB, Santiago BM, Cavalcanti YW, de Almeida LFD. The use of mouthguards and prevalence of dento-alveolar trauma among athletes: A systematic review and meta-analysis. *Dent Traumatol.* 2019;35:54-72. doi: 10.1111/edt.12441.

7. Chisholm DA, Black AM, Palacios-Derflingher L, Eliason PH, Schneider KJ, Emery CA, Hagel BE. Mouthguard use in youth ice hockey and the risk of concussion: nested case-control study of 315 cases. *Br J Sports Med.* 2020;54:866-70. doi: 10.1136/bjsports-2019-101011.
8. Carvalho VF, Soares PB, Verissimo C, Pessoa RS, Versluis A, Soares CJ. Mouthguard Biomechanics for Protecting Dental Implants from Impact: Experimental and Finite Element Impact Analysis. *Int J Oral Maxillofac Implants.* 2018;33:335-43. doi: 10.11607/jomi.5803.
9. Tribst JPM, de Oliveira Dal Piva AM, Borges ALS, Bottino MA. Influence of custom-made and stock mouthguard thickness on biomechanical response to a simulated impact. *Dent Traumatol.* 2018;34:429-37. doi: 10.1111/edt.12432.
10. de Melo C, Resende JB, Lozada MIT, Mendoza LCL, Ribeiro MTH, Soares PBF, Soares CJ. Effect of surface treatment of ethylene vinyl acetate on the delamination of custom-fitted mouthguards. *Dent Traumatol.* 2023;39:324-32. doi: 10.1111/edt.12826.
11. Veríssimo C, Bicalho AA, Soares PB, Tantbirojn D, Versluis A, Soares CJ. The effect of antagonist tooth contact on the biomechanical response of custom-fitted mouthguards. *Dent Traumatol.* 2017;33:57-63. doi: 10.1111/edt.12284.
12. Abe M, Sugimoto A, Togawa H, Gonda T, Maeda Y, Ikebe K. Longitudinal changes in mouthguard fit: Reliability of an evaluation method. *Dent Traumatol.* 2020;36:203-6. doi: 10.1111/edt.12522.
13. Mizuhashi F, Koide K. Appropriate fabrication method for pressure-formed mouthguards using ethylene vinyl acetate sheets. *Dent Traumatol.* 2018;34:46-50. doi: 10.1111/edt.12373.

14. Abbott PV, Tewari N, O'Connell AC, Mills SC, Stasiuk H, Roettger M, Levin L. The International Association of Dental Traumatology (IADT) and the Academy for Sports Dentistry (ASD) guidelines for prevention of traumatic dental injuries: Part 3: Mouthguards for the prevention of dental and oral trauma. *Dent Traumatol*. 2024 Feb;40 Suppl 1:7-9. <https://doi.org/10.1111/edt.12925>
15. Westerman B, Stringfellow PM, Eccleston JA. EVA mouthguards: how thick should they be? *Dent Traumatol*. 2002;18:24-7. doi: 10.1034/j.1600-9657.2002.180103.x.
16. Verissimo C, Costa PV, Santos-Filho PC, Tantbirojn D, Versluis A, Soares CJ. Custom-Fitted EVA Mouthguards: what is the ideal thickness? a dynamic finite element impact study. *Dent Traumatol*. 2016;32:95-102. doi: 10.1111/edt.12210.
17. Doğan SSA, Doğan Ö, Doğan Ö, Başkurt NA. Protective potential of different mouthguard thicknesses against perianaesthetic dental trauma: a patient specific finite element study. *Comput Methods Biomech Biomed Engin*. 2023;17:1-11. doi: 10.1080/10255842.2023.2247515.
18. Flores-Figueiras C, Zamora-Olave C, Willaert E, Martinez-Gomis J. Effect of thickness and occlusal accommodation on the degree of satisfaction with mouthguard use among water polo players: A randomized crossover trial. *Dent Traumatol*. 2020;36:670-9. doi: 10.1111/edt.12583.
19. Takahashi M, Bando Y. Effect on thickness of a single-layer mouthguard of positional relationship between suction port of the vacuum forming device and the model. *Dent Traumatol*. 2021;37:502-9. doi: 10.1111/edt.12646.
20. Takahashi M, Bando Y. Prioritizing model trimming to prevent thinning during mouthguard thermoforming: Influence of increased height associated with an acute model angle. *Dent Traumatol*. 2023;39:11-8. doi: 10.1111/edt.12795.

21. Del Rossi G, Leyte-Vidal MA. Fabricating a better mouthguard. Part I: factors influencing mouthguard thinning. *Dent Traumatol.* 2007;23:149-54. doi: 10.1111/j.1600-9657.2006.00436.x.
22. Kalra A, Harrington C, Minhas G, Papageorgiou SN, Cobourne MT. Wearability and preference of mouthguard during sport in patients undergoing orthodontic treatment with fixed appliances: a randomized clinical trial. *Eur J Orthod.* 2022;44:101-9. doi: 10.1093/ejo/cjab062.
23. Karaganeva R, Pinner S, Tomlinson D, Burden A, Taylor R, Yates J, Winwood K. Effect of mouthguard design on retention and potential issues arising with usability in sport. *Dent Traumatol.* 2019;35:73-9. doi: 10.1111/edt.12446.
24. Mizuhashi F, Koide K. Vacuum-formed mouthguard fabrication to obtain proper fit using notched sheet. *Dent Traumatol.* 2019;35:204-11. doi: 10.1111/edt.12463.
25. Parker K, Marlow B, Patel N, Gill DS. A review of mouthguards: effectiveness, types, characteristics and indications for use. *Br Dent J.* 2017;222:629-33. doi: 10.1038/sj.bdj.2017.365.
26. Tribst JPM, Dal Piva AMO, Bottino MA, Kleverlaan CJ, Koolstra JH. Mouthguard use and TMJ injury prevention with different occlusions: A three-dimensional finite element analysis. *Dent Traumatol.* 2020;36:662-669. doi: 10.1111/edt.12577.
27. Rondón AKA, Lozada MIT, Soares PBF, Raposo LHA, Soares CJ. Effect of different materials for conventional and 3D-printed models on the mechanical properties of ethylene-vinyl acetate utilized for fabricating custom-fit mouthguards. *Dent Traumatol.* 2023;00:1-8. doi: 10.1111/edt.12912.
28. Balhaddad AA, Garcia IM, Mokeem L, Alsaifi R, Majeed-Saidan A, Albagami HH, Khan AS, Ahmad S, Collares FM, Della Bona A, Melo MAS. Three-dimensional (3D) printing

- in dental practice: Applications, areas of interest, and level of evidence. *Clin Oral Investig.* 2023;27:2465-81. doi: 10.1007/s00784-023-04983-7.
29. Joda T, Matthisson L, Zitzmann NU. Impact of Aging on the Accuracy of 3D-Printed Dental Models: An In Vitro Investigation. *J Clin Med.* 2020;9:1436. doi: 10.3390/jcm9051436.
30. Andjela L, Abdurahmanovich VM, Vladimirovna SN, Mikhailovna GI, Yurievich DD, Alekseevna MY. A review on Vat Photopolymerization 3D-printing processes for dental application. *Dent Mater.* 2022;38:284-296. doi: 10.1016/j.dental.2022.09.005.
31. de Paris Matos T, Wambier LM, Favoreto MW, Rezende CEE, Reis A, Loguercio AD, Gonzaga CC. Patient-related outcomes of conventional impression making versus intraoral scanning for prosthetic rehabilitation: A systematic review and meta-analysis. *J Prosthet Dent.* 2023;130(1):19-27. doi: 10.1016/j.prosdent.2021.08.022.
32. Rhee YK, Huh YH, Cho LR, Park CJ. Comparison of intraoral scanning and conventional impression techniques using 3-dimensional superimposition. *J Adv Prosthodont.* 2015;7(6):460-7. doi: 10.4047/jap.2015.7.6.46
33. Sasayama C, Taniuchi H, Takamata T, Kasahara T, Kagiya S, Komeda, K, et al. Microwave oven vulcanizing silicone-based material for sports mouthguards – physical properties and clinical procedures. *Int J Sports Dent.* 2014;7:63–76.
34. Abe M, Sugimoto A, Togawa H, Gonda T, Maeda Y, Ikebe K. Longitudinal changes in mouthguard fit: Reliability of an evaluation method. *Dent Traumatol.* 2020;36:203–206. <https://doi.org/10.1111/edt.12522>
35. Tanabe G, Churei H, Wada T, Takahashi H, Uo M, Ueno T. The influence of temperature on sheet lamination process when fabricating mouthguard on dental thermoforming machine. *J Oral Sci.* 2020;62:23–7. doi: 10.2334/josnusd.18-0421.

36. Takahashi M, Bando Y. In vitro study of how the undercut amount on the model labial side affects the reduction rate of laminated mouthguard thickness. *Dent Traumatol.* 2023;39:206-213. doi: 10.1111/edt.12820.
37. Takahashi M, Bando Y. Effect of acute angle model on mouthguard thickness with the thermoforming method and moving the model position just before fabrication. *Dent Traumatol.* 2021;37:138-144. doi: 10.1111/edt.12603.
38. Costa PVM, Firmiano TC, Borges GA, Dantas RP, Veríssimo C. The effect of the simulated aging by thermocycling on the elastic modulus of ethylene-vinyl acetate brands and stress/strain development during an impact: An in vitro and 3D-FEA analysis. *Dent Traumatol.* 2024;40:204-212. doi: 10.1111/edt.12896.
39. Horri A, Shojaepoor R, Jahanimoghadam F, Bahador A, Pouradeli S. Effect of mouthguard on sport-related orofacial injuries in adolescents in Kerman. *Iran IJBR.* 2016;7:2228–34.
40. Gao L, McCarthy TJ. Contact angle hysteresis explained. *Langmuir.* 2006;22:6234–7. doi: 10.1021/la060254j.
41. Tiwari U, Mishra V, Bhalla A, Singh N, Jain SC, Garg H, et al. Fiber Bragg grating sensor for measurement of impact absorption capability of mouthguards. *Dent Traumatol.* 2011;27:263–8. doi: 10.1111/j.1600-9657.2011.00998.
42. Guérard S, Barou JL, Petit J, Poisson P. Characterization of mouthguards: impact performance. *Dent Traumatol.* 2017;33:281–7. doi: 10.1111/edt.12329.
43. Lo Giudice R, Lizio A, Cervino G, Fabiana N, Francesco P, Ausiello P, Cicciù M. The Horizontal Root Fractures. Diagnosis, Clinical Management and Three-Year Follow-Up. *Open Dent J.* 2018;12:687-695. doi: 10.2174/1745017901814010687.

44. Francisco SS, Filho FJ, Pinheiro ET, Murrer RD, de Jesus Soares A. Prevalence of traumatic dental injuries and associated factors among Brazilian schoolchildren. *Oral Health Prev. Dent.* 2013;11:31-8. doi: 10.3290/j.ohpd.a29373.

TABLE 1 Classification of the fracture modes.

Models	I non fracture	II coronal fracture	III Fracture at the alveolar bone	IV fracture at the lingual root
3D-printed model mouthguard	10	-	-	-
Plaster model – mouthguard	10	-	-	-
Without mouthguard	5	-	4	1

FIGURES

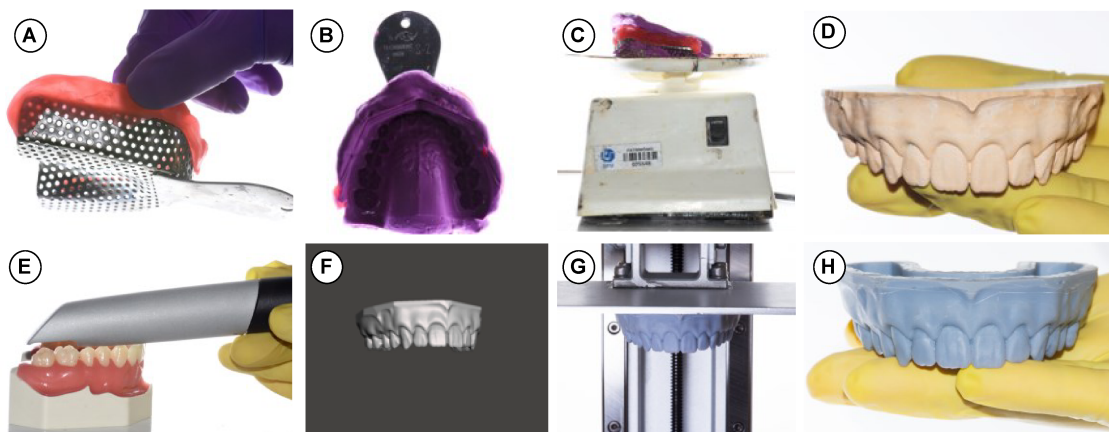


FIGURE 1. Specimen Fabrication: (A) Beading wax; (B) Alginate molding; (C) Plaster vibrator used to remove air bubbles from the gypsum; (D) Gypsum model; (E) Scanned with a 3D intraoral scanner (Straumann, Virtuo Vivo); (F) The stereolithography (STL) file imported to the workflow software (Meshmixer 2017, Autodesk); (G) 3D printer (Anycubic Photon Mono X, Anycubic); (H) 3D-printed model.





FIGURE 2. Mouthguard Fabrication: (A) EVA sheets (Bioart Dental Equipment); (B) The first EVA plate was allowed to cool; (C) Finishing of the edge; (D) Polishing with Scotch Brite brushes; (E) Application of Resin monomer (VIPI Flash, VIPI Odonto Products, Pirassununga, Brazil) (F) Application of Resin monomer (VIPI Flash, VIPI Odonto Products, Pirassununga, Brazil) on the first EVA plate; (G) Application of Resin monomer on the second EVA plate; (H) Plasticization of the second EVA plate; (I) Finishing and polishing of the mouthguard.

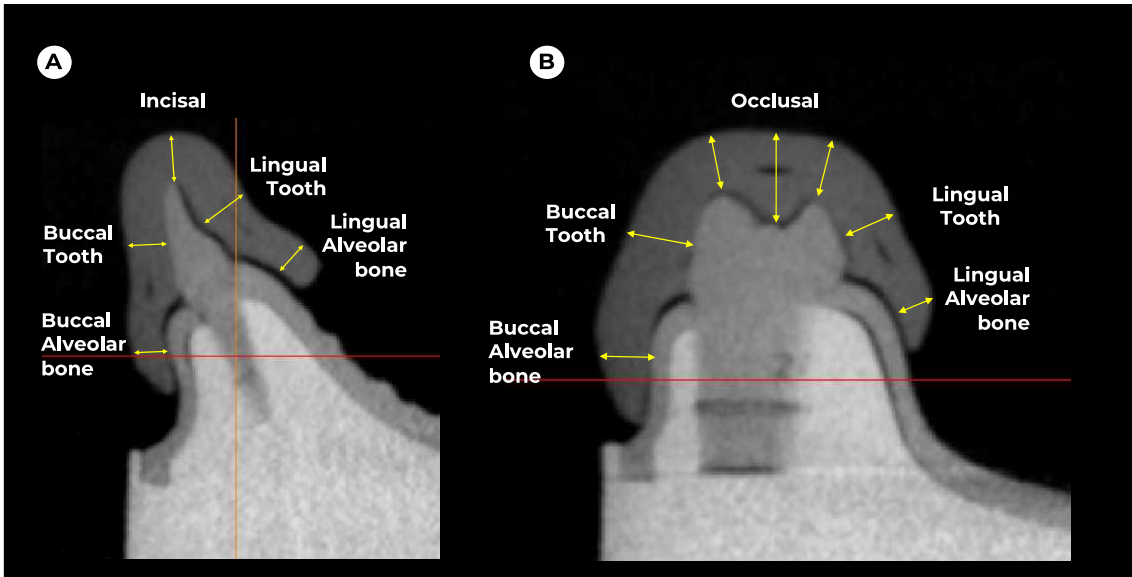


FIGURE 3. MTG thickness measurements: (A) CBCT image of maxillary central incisor was used for MTG thickness measurements at five locations of the anterior segment; (B) CBCT image of maxillary first molar with mouthguard for thickness measurement at seven locations.

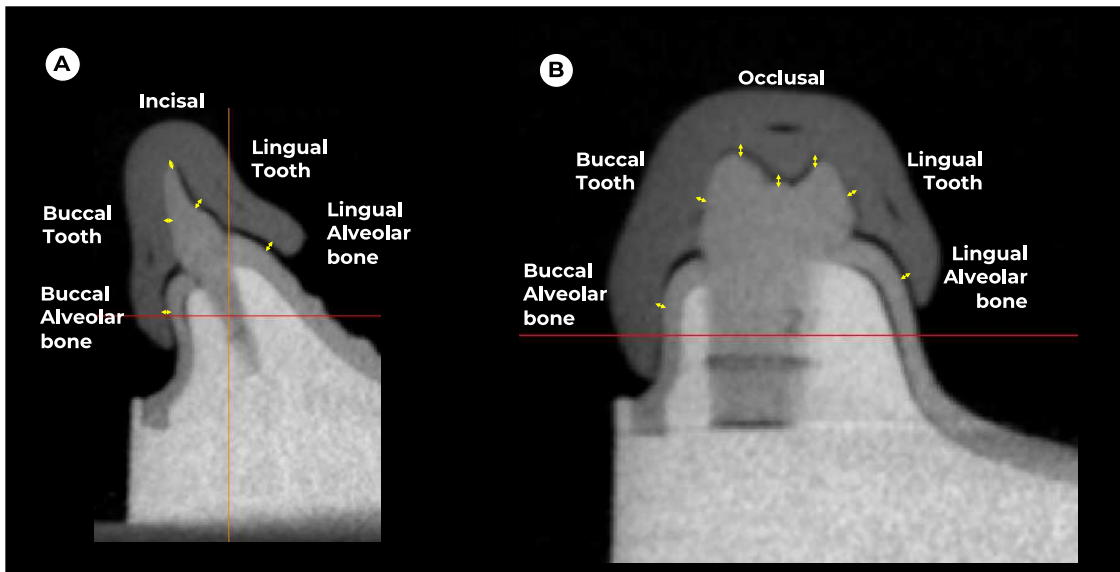


FIGURE 4. Mouthguard adaptation measurements: (A) CBCT image of maxillary central incisor with mouthguard, for adaptation measurement at the five locations for the anterior region; (B) CBCT image of maxillary first molar with mouthguard for adaptation measurement at seven locations.

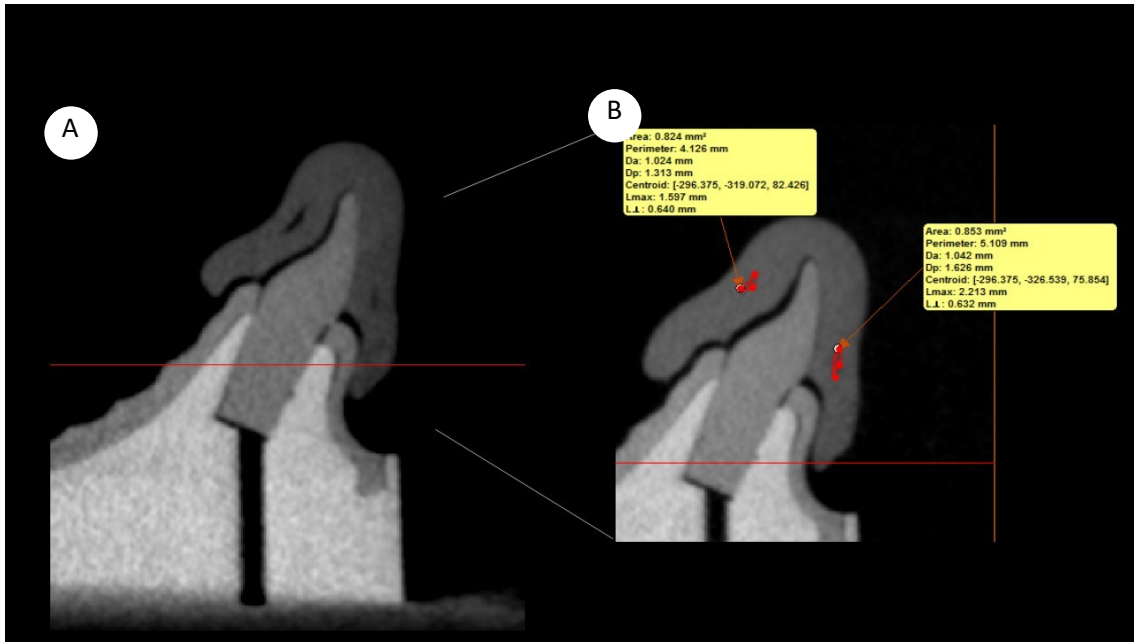


FIGURE 5. Mouthguard Void area Measurements: (A) CT-tomography image of maxillary central incisor with mouthguard, (B) Mouthguard void area measurements between the layers of EVA.



FIGURE 6. Impact Test: (A) Adaptation of the strain-gauge on the palatal surface maxillary central incisor; (B) Impact simulation without mouthguard; (C) Impact simulation with mouthguard, (D) Impact simulation on upper central incisor with strain-gauge on the palatal aspect, (E) Root fracture post-impact without mouthguard.

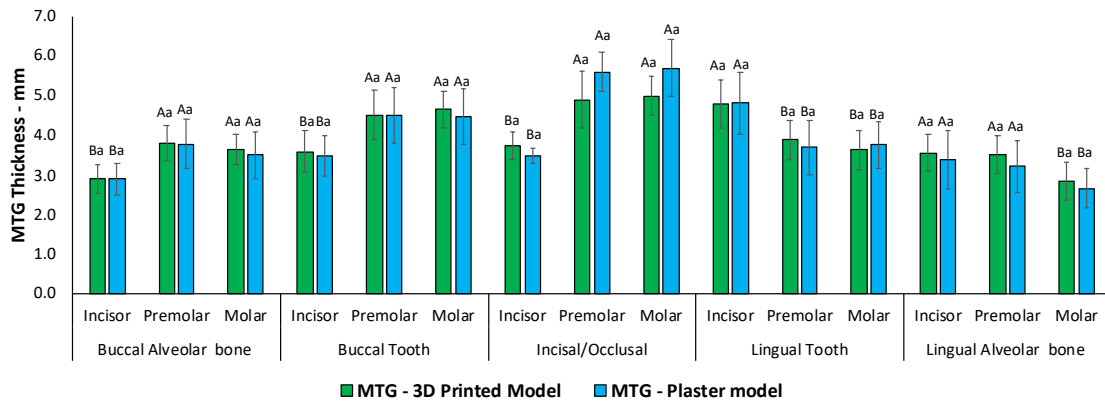


FIGURE 7. Mean of the thickness (mm) and standard deviation values of the mouthguards at different locations of the 3D-printed model and plaster model.

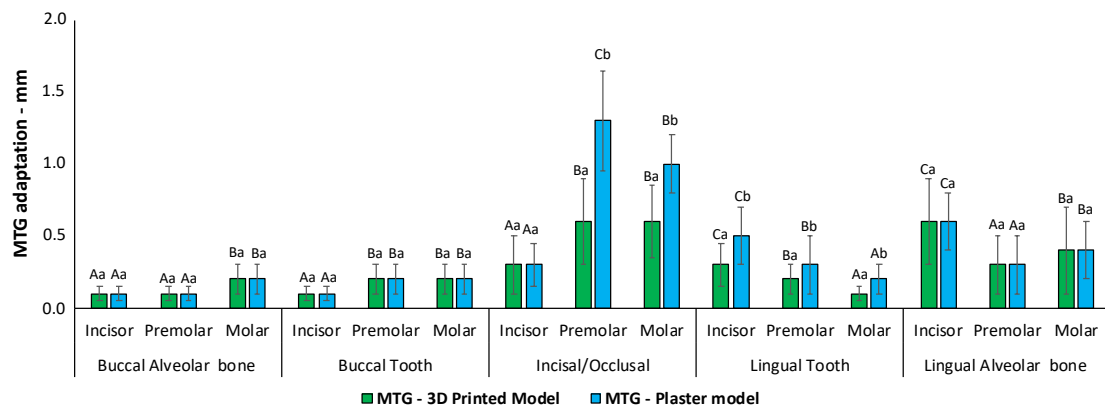


FIGURE 8. Mean of the Adaptation (mm) and standard deviation values of the mouthguards at different locations of the 3D-printed model and plaster model.

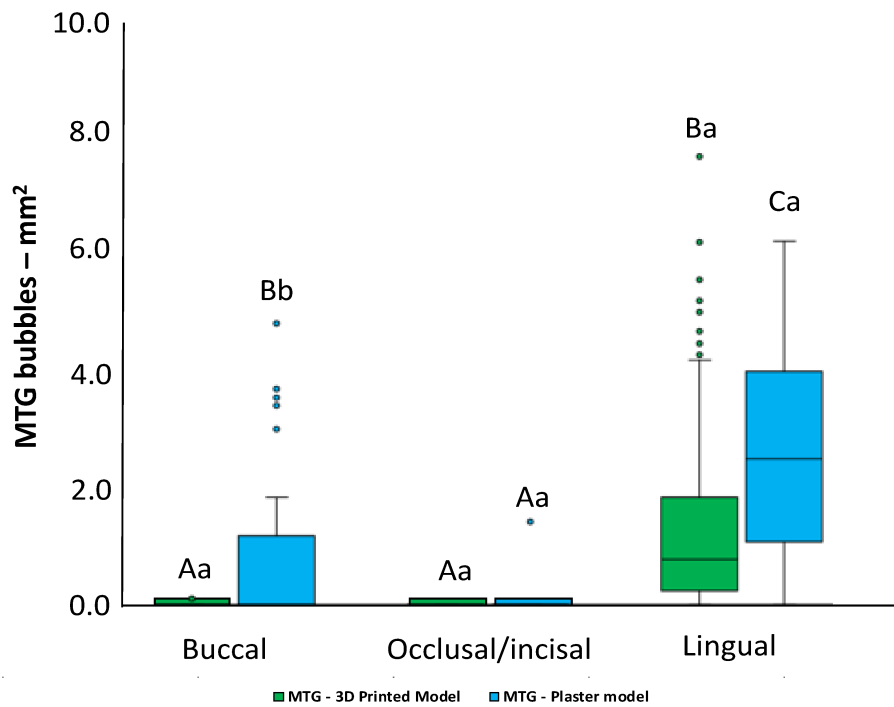


FIGURE 9. Mean of the void areas (mm<sup>2</sup>) and standard deviations of the mouthguards at different locations of the 3D-printed model and plaster model.

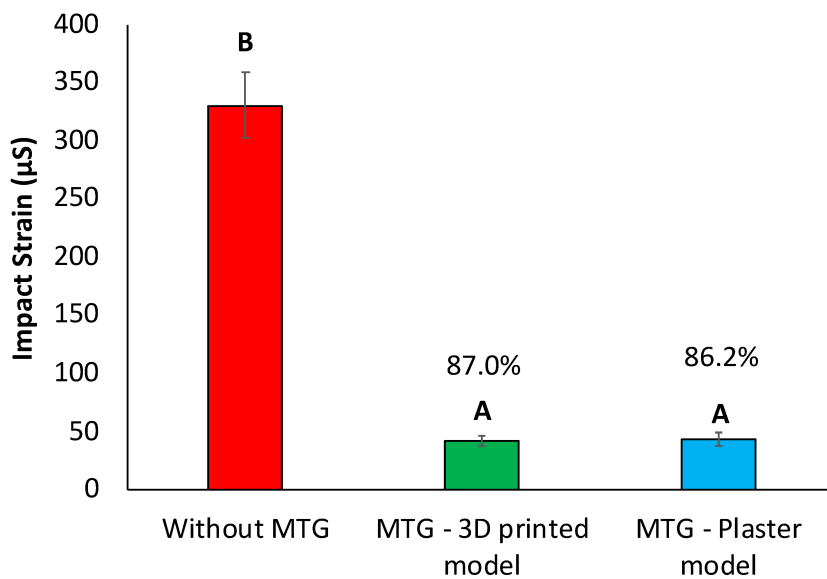


FIGURE 10. Mean of the strain peak (µS) and standard deviation values during the horizontal impact at 30° using the pendulum device of the specimen without mouthguard, with 3D-printed model, and mouthguard plaster model.

# Considerações Gerais

---

A partir do desenvolvimento dos dois estudos laboratoriais in vitro descritos anteriormente, podemos extrair as principais reflexões sobre o uso do fluxo digital na confecção de protetores bucais customizados:

- A interação do modelo de resina impressa 3D sem tratamento de superfície comprometeu as características de superfície e propriedades mecânicas do EVA usado para confecção de protetores bucais customizados;
- Modelos confeccionados em gesso dental tipo IV reforçado com resina alterou as características de superfície e propriedades mecânicas do EVA;
- A aplicação de camada de gel transparente solúvel em água durante o pós-cura sobre modelo de resina impressa 3D eliminou o efeito negativo nas características de superfície e propriedades mecânicas do EVA, resultando em um desempenho semelhante ao modelo de gesso dental tipo IV convencional;
- O uso de protetores bucais customizados reduziu significativamente os valores de deformação dos dentes durante o impacto horizontal em comparação com os dentes impactados sem protetores bucais customizados;
- Os protetores bucais customizados produzidos utilizando tanto sobre modelos de gesso (87,0%), como modelos de resina impressa 3D com tratamento de superfície com gel hidrossolúvel (86,2%) apresentaram alta absorção de choque em comparação com o impacto sem o uso de protetores bucais customizados;
- Pequenas quantidades de bolhas foram observadas entre as duas camadas de EVA, as quais não tiveram efeito significativo no desempenho biomecânico dos protetores bucais customizados;
- Protetores bucais customizados confeccionados sobre modelos de resina impressa 3D com tratamento de superfície com gel hidrossolúvel mostrou melhor adaptação que o protetores bucais customizados confeccionados sobre modelos de gesso nas localizações dos dentes incisais/oclusais e linguais, porém essa melhora na adaptação não refletiu em melhor desempenho biomecânico;
- A impressão digital e a confecção de modelos impressos em resina 3D mostraram ser uma alternativa viável para produzir Protetores bucais customizados com

desempenho semelhante ao padrão ouro produzido usando protocolos de moldagem convencional e modelo de gesso.

# Referências

---

1. Petti S, Glendor U, Andersson L. World traumatic dental injury prevalence and incidence, a meta-analysis- one billion living people have had traumatic dental injuries. *Dent Traumatol.* 2018;34(2):71-86. <https://doi.org/10.1111/edt.12389>
2. Atif M, Tewari N, Reshikesh M, Chanda A, Mathur VP, Morankar R. Methods and applications of finite element analysis in dental trauma research: A scoping review. *Dent Traumatol.* 2024 Jan 26. <https://doi.org/10.1111/edt.12933>
3. Oliveira Werlich M, Honnef LR, Silva Bett JV, Domingos FL, Pauletto P, Dulcineia Mendes de Souza B, et al. Prevalence of dentofacial injuries in contact sports players: A systematic review and meta-analysis. *Dent Traumatol.* 2020;36:477-88. <https://doi.org/10.1111/edt.12556>
4. Fernandes LM, Neto JCL, Lima TFR, Magno MB, Santiago BM, Cavalcanti YW, de Almeida LFD. The use of mouthguards and prevalence of dento-alveolar trauma among athletes: A systematic review and meta-analysis. *Dent Traumatol.* 2019 Feb;35(1):54-72. <https://doi.org/10.1111/edt.12441>
5. Doğan SSA, Doğan Ö, Doğan Ö, Başkurt NA. Protective potential of different mouthguard thicknesses against perianaesthetic dental trauma: a patient specific-finite element study. *Comput Methods Biomech Biomed Engin.* 2023;17:1-11. <https://doi.org/10.1080/10255842.2023.2247515>
6. Bragança GF, Vilela ABF, Soares PBF, Tantbirojn D, Versluis A, Soares CJ. Influence of ceramic veneer thickness and antagonist on impact stresses during dental trauma with and without a mouthguard assessed with finite element analysis. *Dent Traumatol.* 2021;37:215-22. <https://doi.org/10.1111/edt.12631>
7. Veríssimo C, Bicalho AA, Soares PB, Tantbirojn D, Versluis A, Soares CJ. The effect of antagonist tooth contact on the biomechanical response of custom-fitted mouthguards. *Dent Traumatol.* 2017;33:57-63. <https://doi.org/10.1111/edt.12284>



8. Tanaka Y, Tsugawa T, Maeda Y. Effect of mouthguards on impact to the craniomandibular complex. *Dent Traumatol.* 2017 Feb;33(1):51-56. doi: 10.1111/edt.12283. <https://doi.org/10.1111/edt.12283>
9. Vilela ABF, Soares PBF, de Oliveira FS, Garcia-Silva TC, Estrela C, Versluis A, Soares CJ. Dental trauma on primary teeth at different root resorption stages-A dynamic finite element impact analysis of the effect on the permanent tooth germ. *Dent Traumatol.* 2019 Apr;35(2):101-108. doi: 10.1111/edt.12460. <https://doi.org/10.1111/edt.12460>
10. Roberts HW. Sports mouthguard overview: materials, fabrication techniques, existing standards, and future research needs. *Dent Traumatol.* 2023;39(2):101-8. <https://doi.org/10.1111/edt.12809>
11. de Melo C, Resende JB, Lozada MIT, Mendoza LCL, Ribeiro MTH, Soares PBF, Soares CJ. Effect of surface treatment of ethylene vinyl acetate on the delamination of custom-fitted mouthguards. *Dent Traumatol.* 2023;39:324-32. <https://doi.org/10.1111/edt.12826>
12. Verissimo C, Costa PV, Santos-Filho PC, Fernandes-Neto AJ, Tantbirojn D, Versluis A, Soares CJ. Evaluation of a dentoalveolar model for testing mouthguards: stress and strain analyses. *Dent Traumatol.* 2016 Feb;32(1):4-13. doi: 10.1111/edt.12197. <https://doi.org/10.1111/edt.12197>
13. Costa PVM, Firmiano TC, Borges GA, Dantas RP, Verissimo C. The effect of the simulated aging by thermocycling on the elastic modulus of ethylene-vinyl acetate brands and stress/strain development during an impact: An in vitro and 3D-FEA analysis. *Dent Traumatol.* 2024 Apr;40(2):204-212. doi: 10.1111/edt.12896. <https://doi.org/10.1111/edt.12896>
14. Abe M, Sugimoto A, Togawa H, Gonda T, Maeda Y, Ikebe K. Longitudinal changes in mouthguard fit: reliability of an evaluation method. *Dent Traumatol.* 2020;36:203-6. <https://doi.org/10.1111/edt.12522>
15. Duddy FA, Weissman J, Lee RA Sr, Paranjpe A, Johnson JD, Cohenca N. Influence of different types of mouthguards on strength and performance of collegiate athletes: a controlled-randomized trial. *Dent Traumatol.* 2012;28:263-7. <https://doi.org/10.1111/j.1600-9657.2011.01106.x>

16. Maeda M, Takeda T, Nakajima K, Shibusawa M, Kurokawa K, Shimada A, Takayama K, Ishigami K. In search of necessary mouthguard thickness. Part 1: From the viewpoint of shock absorption ability. *Nihon Hotetsu Shika Gakkai Zasshi*. 2008 Apr;52(2):211-9. doi: 10.2186/jjps.52.211. <https://doi.org/10.2186/jjps.52.211>
17. Firmiano TC, de Oliveira AA, Costa PVM, Cardoso LS, Pereira RD, Veríssimo C. Influence of different ethylene-vinyl acetate brands used for custom-fitted mouthguard fabrication on the stress and strain during an impact. *Dent Traumatol*. 2022 Oct;38(5):431-438. doi: 10.1111/edt.12746 <https://doi.org/10.1111/edt.12746>
18. Tribst JPM, de Oliveira Dal Piva AM, Borges ALS, Bottino MA. Influence of custom-made and stock mouthguard thickness on biomechanical response to a simulated impact. *Dent Traumatol*. 2018;34:429-37. <https://doi.org/10.1111/edt.12432>
19. Coto NP, Dias RB, Costa RA, Antoniazzi TF, Carvalho EP. Mechanical behavior of ethylene vinyl acetate copolymer (EVA) used for fabrication of mouthguards and interocclusal splints. *Braz Dent J*. 2007;18:324- 8 <https://doi.org/10.1590/S0103-64402007000400010>
20. Mizuhashi F, Koide K. Appropriate fabrication method for pressure- formed mouthguards using ethylene vinyl acetate sheets. *Dent Traumatol*. 2018;34:46-50 <https://doi.org/10.1111/edt.12373>
21. Kong, L., Li, Y. & Liu, Z. Digital versus conventional full-arch impressions in linear and 3D accuracy: a systematic review and meta-analysis of in vivo studies. *Clin Oral Invest* 26, 5625-5642 (2022). <https://doi.org/10.1007/s00784-022-04607-6>
22. Albanchez-González MI, Brinkmann JC, Peláez-Rico J, López-Suárez C, Rodríguez-Alonso V, Suárez-García MJ. Accuracy of Digital Dental Implants Impression Taking with Intraoral Scanners Compared with Conventional Impression Techniques: A Systematic Review of In Vitro Studies. *Int J Environ Res Public Health*. 2022 Feb 11;19(4):2026. <https://doi.org/10.3390/ijerph19042026>
23. Papaspyridakos, P., Hirayama, H., Chen, C.J., Ho, C.H., Chronopoulos, V. & Weber, H.P.(2015) Full-arch implant fixed prostheses: a comparative study on the effect of connection type and impression technique on accuracy of fit. *Clinical Oral Implants Research* 27: 1099-1105. <https://doi.org/10.1111/clr.12695>

24. Amin S, Weber HP, Finkelman M, El Rafie K, Kudara Y, Papaspyridakos P. Digital vs. conventional full-arch implant impressions: a comparative study. *Clin. Oral Impl. Res.* 28, 2017, 1360-136. <https://doi.org/10.1111/clr.12994>